

2006

## Design of a quick-release mechanism for a C-130 aircraft sensor platform

Seth D. Lucey  
*West Virginia University*

Follow this and additional works at: <https://researchrepository.wvu.edu/etd>

---

### Recommended Citation

Lucey, Seth D., "Design of a quick-release mechanism for a C-130 aircraft sensor platform" (2006).  
*Graduate Theses, Dissertations, and Problem Reports*. 1736.  
<https://researchrepository.wvu.edu/etd/1736>

This Thesis is protected by copyright and/or related rights. It has been brought to you by the The Research Repository @ WVU with permission from the rights-holder(s). You are free to use this Thesis in any way that is permitted by the copyright and related rights legislation that applies to your use. For other uses you must obtain permission from the rights-holder(s) directly, unless additional rights are indicated by a Creative Commons license in the record and/ or on the work itself. This Thesis has been accepted for inclusion in WVU Graduate Theses, Dissertations, and Problem Reports collection by an authorized administrator of The Research Repository @ WVU. For more information, please contact [researchrepository@mail.wvu.edu](mailto:researchrepository@mail.wvu.edu).

Design of a Quick-Release Mechanism for a  
C-130 Aircraft Sensor Platform

Seth D. Lucey

A thesis submitted to the College of Engineering and Mineral Resources at West Virginia  
University

In partial fulfillment of the requirements for the degree of  
Master of Science  
in  
Mechanical Engineering

James Smith, PhD., Chair  
Kenneth Means, PhD.  
Gregory Thompson, PhD.

Department: Mechanical and Aerospace Engineering  
Major: Mechanical Engineering

West Virginia University  
Morgantown, WV  
2006

Keywords: C-130, Pallet Design, Quick Attach, Optimization  
Copyright Seth D. Lucey, 2006. All rights reserved.

## ABSTRACT

### Design of a Quick-Release Mechanism for a C-130 Aircraft Sensor Platform

Seth D. Lucey

The development of a standardized sensor pallet system for a C-130 aircraft was conceived by the Center for Industrial Research Applications at West Virginia University to assist in counterdrug reconnaissance activities within the United States. The system has been completed and is now being optimized for various uses in addition to counterdrug reconnaissance. It is sought to have the sensor carriers/housings easily interchangeable so that they may be switched in the field by operators rather than in the hangar by technicians. The design parameters were established by the National Guard mission requirements and by the limitations of the C-130 aircraft. These limitations include using Commercial off the Shelf (COTS) and Government off the Shelf (GOTS) components when developing the system that must be universal on all C-130 aircraft variants B thru H. The following work describes the design process and engineering analysis of this “quick-release” mechanism design.

<b>Table of Contents</b>	<b>Page #</b>
<b>Title Page</b>	<b>i</b>
<b>Abstract</b>	<b>ii</b>
<b>Table of Contents</b>	<b>iii</b>
<b>Figures Listed</b>	<b>iv</b>
<b>Tables Listed</b>	<b>vii</b>
<b>Acknowledgements</b>	<b>viii</b>
<b>Personal Acknowledgments</b>	<b>viii</b>
<b>1.0 Introduction</b>	<b>1</b>
<b>2.0 Literature Review</b>	<b>6</b>
2.1 Quick-Attachment Review	<b>6</b>
2.2 Finite Element Analysis Review	<b>14</b>
<b>3.0 Quick-Release Design</b>	<b>16</b>
<b>4.0 Component Analysis</b>	<b>34</b>
<b>5.0 Results and Conclusion</b>	<b>54</b>
<b>6.0 Future Work</b>	<b>55</b>
<b>7.0 References</b>	<b>56</b>
<b>Appendix A</b>	<b>59</b>
<b>Appendix B</b>	<b>63</b>

<b>Figures Listed</b>	<b>Page #</b>
Figure 1: Placement of Sensor Platform and Operator Station on C-130	<b>1</b>
Figure 2: Current Pod / Arm Arrangement	<b>3</b>
Figure 3: Original Tool Attachment	<b>7</b>
Figure 4: Patent Number 3,606,052 Dual	<b>8</b>
Figure 5: Patent Number 6,851,916 Toro	<b>9</b>
Figure 6: Patent Number 4,030,624 Massey Ferguson	<b>10</b>
Figure 7: Patent Number 5,836,734 Deere	<b>11</b>
Figure 8: Bobcat Quick Attach	<b>12</b>
Figure 9: Patent Number 4,812,103 Case	<b>12</b>
Figure 10: Quick Release System	<b>16</b>
Figure 11: Exploded View of Components	<b>17</b>
Figure 12: Space Allowed for Attachment Device	<b>19</b>
Figure 13: Comparison of Unlocked/Locked Positions	<b>21</b>
Figure 14: Pod and Arms with Quick Attach Locked	<b>22</b>
Figure 15: Diagram of 4-bar Slider-Crank Mechanism	<b>23</b>
Figure 16: Geometry of Mechanism	<b>24</b>
Figure 17: Spring Pin	<b>26</b>
Figure 18: Mechanism in the Unlocked, Center, and Locked Positions	<b>27</b>
Figure 19: Spring-Loaded Link in the Unlocked, Center, and Locked Positions	<b>27</b>
Figure 20: Angle of Rotation of Handle and Distance of Translation of Pin	<b>29</b>
Figure 21: Sensor Pod Frame	<b>30</b>

<b>Figures Listed</b>	<b>Page #</b>
Figure 22: Sensor Pod Frame with Attachment Brackets	<b>30</b>
Figure 23: Pod Attachment Bracket	<b>31</b>
Figure 24: Arm, Frame, and Latch Mechanism Assembly	<b>33</b>
Figure 25: Loading on Pin at Mid-Deployment	<b>35</b>
Figure 26: Mechanical Advantage Force Comparison	<b>37</b>
Figure 27: Load Applied to Pod Attachment Bracket in the Deployed Position	<b>38</b>
Figure 28: Load Applied to the Pod Attachment Bracket in the Mid-Deployment Position	<b>39</b>
Figure 29: Load Applied to the Pod Attachment Bracket in the Stowed Position	<b>40</b>
Figure 30: Load Applied to the Arm Frame in the Deployed Position	<b>41</b>
Figure 31: Load Applied to the Arm Frame in the Mid-Deployment Position	<b>41</b>
Figure 32: Load Applied to the Arm Frame in the Stowed Position	<b>42</b>
Figure 33: Load Applied to the Lock Pin in the Mid-Deployment Position	<b>43</b>
Figure 34: Load Applied to the Female Component of the Spring Link in the Latched Position	<b>44</b>
Figure 35: Load Applied to the Male Component of the Spring Link in the Latched Position	<b>45</b>
Figure 36: Load Applied to the Handle in the Latched Position	<b>46</b>
Figure 37: Goodman Diagram of Pod Attachment Bracket	<b>51</b>
Figure 38: Goodman Diagram of Arm Frame	<b>52</b>
Figure 39: Goodman Diagram of Lock Pin	<b>52</b>
Figure 40: Goodman Diagram of Spring Link	<b>53</b>
Figure 41: Goodman Diagram of Handle	<b>53</b>

<b>Figures Listed</b>	<b>Page #</b>
Figure 42: Quick-Release System	<b>54</b>
Figure 43: Analysis of Pod Attachment Bracket in the Deployed Position	<b>64</b>
Figure 44: Analysis of Pod Attachment Bracket in the Mid-Deployment Position	<b>65</b>
Figure 45: Analysis of Pod Attachment Bracket in the Stowed Position	<b>66</b>
Figure 46: Analysis of Arm Frame in the Deployed Position	<b>67</b>
Figure 47: Analysis of Arm Frame in the Mid-Deployment Position	<b>68</b>
Figure 48: Analysis of Arm Frame in the Stowed Position	<b>69</b>
Figure 49: Analysis of Lock Pin in the Mid-Deployment Position	<b>70</b>
Figure 50: Analysis of Female Component of Spring-Link in the Latched Position	<b>71</b>
Figure 51: Analysis of Male Component of Spring-Link in the Latched Position	<b>72</b>
Figure 52: Analysis of Handle in the Latched Position	<b>73</b>

<b>Tables Listed</b>	<b>Page #</b>
Table 1: Component List	<b>17</b>
Table 2: Component Stress Analysis Results	<b>48</b>
Table 3: Shoulder Bolt Stress Analysis Results	<b>49</b>
Table 4: Modal Analysis Results	<b>50</b>
Table 5: Maximum, Minimum, and Mean Stress Values	<b>51</b>
Table 6: Mechanism Analysis Spreadsheet	<b>60</b>



## **Acknowledgements**

This publication would not have been possible without the dedicated efforts of many individuals. In the spirit of multiple-agency collaboration, the author would like to acknowledge contributions made by Bruce Corso, Arternis System Manager for the Naval Surface Weapons Center, and LTC Michael Thomas, Technical Projects Manager for the NGB-CD. Sincere thanks also to Col. James Hoyer, Col. Frye and all members of the WV-NG and ANG who provided guidance for the planning and development of this technology. Lastly, the West Virginia 130<sup>th</sup> Airlift Wing for their support, professionalism and expertise.

## **Personal Acknowledgements**

This work would not have been possible without the help and support of many individuals. Many people have helped me throughout my engineering education and career. First I would like to thank my parents, Daniel and Colleen Lucey, for their support and encouragement. I would like to thank my advisor and chairperson, Dr. James Smith for taking me on as a graduate student and my committee members Dr. Kenneth Means and Dr. Gregory Thompson for the knowledge, guidance, and encouragement they have contributed. I would like to thank Adam Naternicola for his encouragement to continue my education. I would also like to thank my fellow students Zenovy Wowczuk, Kenny Williams, and Wes Hardin; they have been a pleasure to work with and very supportive during my time as a graduate student.

## **1.0 Introduction**

West Virginia University (WVU) has been tasked with the needs assessment, design and fabrication of a sensor platform that is capable of operating remote sensors for use aboard the C-130 military aircraft [1-13]. WVU has completed design and construction of a transportable roll-on, roll-off sensor pallet(s) that will deploy via the rear cargo door of the aircraft while in flight.

The sensor pallet is built to be carried on the rear ramp of the aircraft, as shown in Figure 1. In flight, the rear doors of the aircraft open and the sensor arm rotates the sensor array outside the rear of the aircraft to perform its mission. In the deployed position the sensor array is positioned underneath the aircraft so as to give it a wide area field-of-view of the ground.

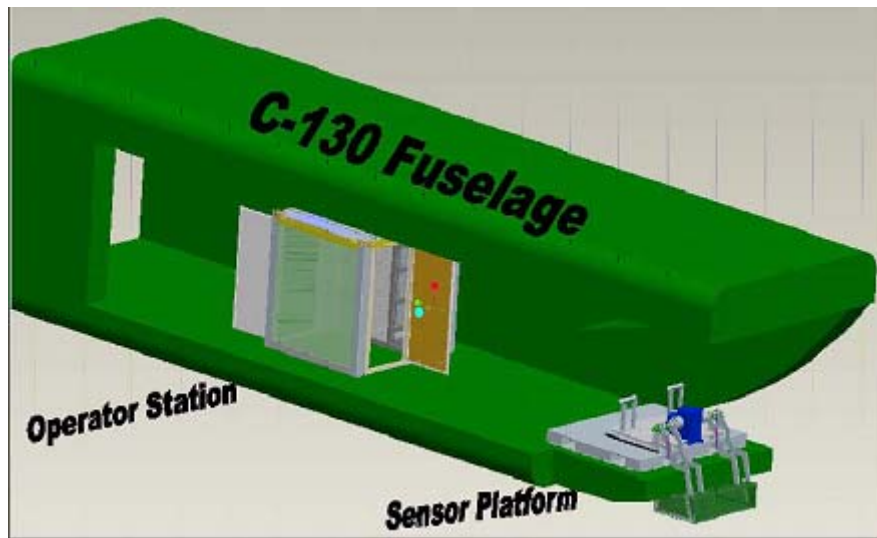


Figure 1: Placement of Sensor Platform and Operator Station on C-130 [13]

The sensor platform holds all the mechanical and electrical components that support and control the motion of the mechanical arms which carry the sensor payload.

The platform can be added to the aircraft as easily as adding a pallet full of supplies, and can be removed from the aircraft easily, carrying all the sensor components, leaving the aircraft in its original state with no modifications.

The electrical components are housed in two sealed, semi-removable aluminum enclosures. The enclosures are weather-tight so that they may be used in various environments. They are removable for quick, easy change-out for maintenance and upgrades. In addition to these two power and control enclosures, there are four sealed, easily detachable enclosures for housing sensor control/data acquisition equipment. The sensor control enclosures are also weather-tight, and have quick-disconnect power supply cables attached to each. The sensor enclosures are designed to be configured and customized by the suppliers/operators of the various sensors. For that reason, they are easily removable for setup, maintenance, mission changes, and data acquisition purposes.

The sensors are carried in a sealed, aluminum enclosure (pod) at the end of the arms. The pod frame is constructed of 5052-H32 aluminum angle, and is covered with 5052 aluminum sheet. The pod incorporates removable sensor-mount surfaces, which are fixed to the pod through vibration isolators. The vibration isolators are COTS items that are available in several load ratings, so the pod can be set up for various sensor payloads.

It is desired to optimize the sensor platform so that it will be as versatile as possible. The C-130 aircraft is available for use to all military agencies, so the sensor platform is to be available and readily set up for each of their respective tasks. In addition to its original intended use (counter-drug missions), the platform can be used for homeland security, border patrol, and surveillance activities. To aid in this capability,

every component should be easily removable and re-attachable for setup, maintenance, and mission changes, like the enclosures described above.

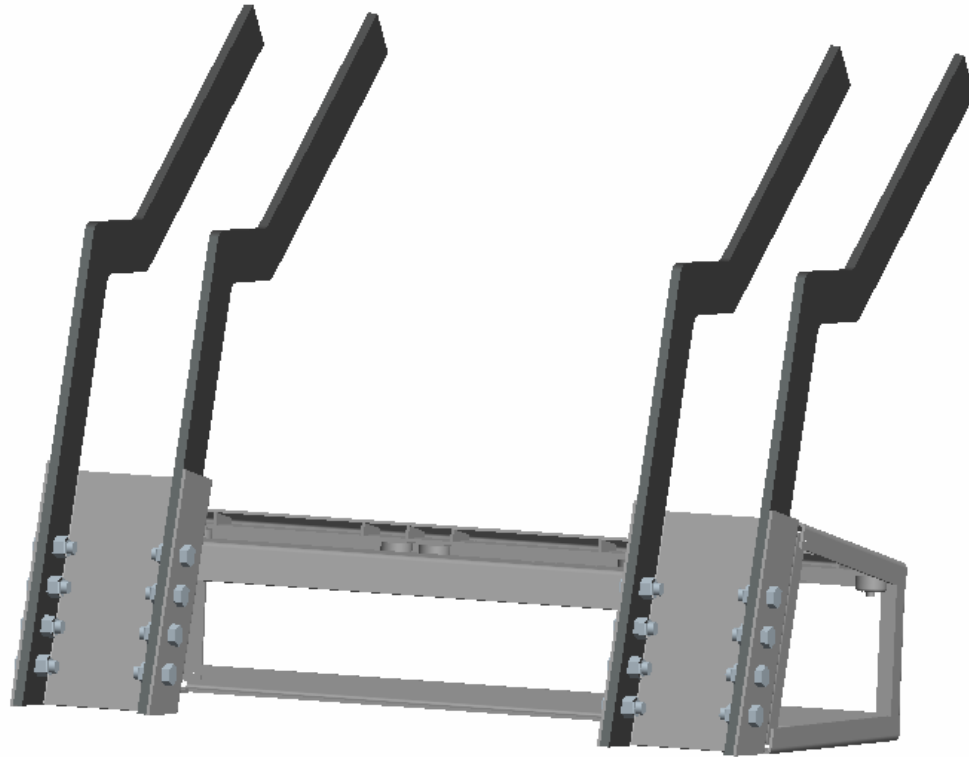


Figure 2: Current Pod / Arm Arrangement

In the current arrangement, the pod is directly attached to the arms with bolts and locknuts as shown in Figure 2. Being bolted to the arms, the pod is not quickly or easily removable, and even less quickly or easily re-attachable. The modification desired here is a quick-release mechanism that will allow easy removal of the pod from the arms, with equally as easy remounting.

The quick-attach system will be similar to those used on agricultural and industrial equipment, especially front loaders, backhoes, and excavators. These machines

are similar to the sensor platform in that they use load-supporting arms that carry various interchangeable implements. The implements are interchangeable for different jobs, which is desirable for the sensor pod. The sensor pod is also roughly the same size and is capable of carrying about the same load as the buckets of the smaller versions of these machines.

Operator requirements pertain to the personnel that must install and remove the pallet and those that must operate the sensors on the pallet during a mission. This requires that the pallet and all of its components must be simple enough to be installed and maintained by existing personnel, and the pallet must mount in the same fashion as standard cargo pallets where the tools and supplies used to maintain the physical pallet must be the same as for other DoD equipment [14].

## **Problem Statement**

It is desired to modify the attachment method of the sensor pod of the Oculus Sensor Deployment System to the arms so that the pod will be easily detachable and re-attachable. This modification will consist of eliminating the bolts that currently fix the pod to the arms and creating a coupling device for interconnecting the pod to the arms.

The design of the coupling device is to be simple, having as few parts and requiring as little space as possible. It must be easy to use, with no special instructions and easy inspection. The components must be Commercial off the Shelf (COTS), Government off the Shelf (GOTS), or easily manufactured. The device must fix the pod to the arms in the same orientation as in the current arrangement. The device must securely support the load of the pod and the sensor array as if it were permanently fixed. A safety factor of 1.5 [15] must be used to account for imperfections in materials, flaws in assembly, material degradation, and uncertainty in load estimates.

## **2.0 Literature Review**

### **2.1 Quick Attachment Review**

In recent years, almost all types of machinery are fitted with easily changeable tools and equipment, e.g., front end loaders and loader tools such as buckets used on today's utility tractors. The changeability of these tools allows the use of one piece of machinery to do the jobs of many, with a simple change of tools.

These loaders and other machines use a variety of techniques to connect the end tools, but all of these techniques are somewhat similar. The different connection mechanisms typically show a progression of improvements made to previous devices, with leading manufacturers having the most refined models. Many manufacturers have merged their designs so that tools are interchangeable. Also, many aftermarket manufacturers have built tools to fit mainline manufacturers' machines.

Most utility equipment is built to either push or lift. Consequently, their attachment mechanisms show these characteristics. The members that push or lift the tool and its load are built with the most strength, while other members are just to hold the attachment to the machine. The machines and tools usually have a large interface area such as a steel plate in the direction of travel for pushing, and large hooks, catches, or channels at the upper sections for lifting. The attachment usually uses pins, bolts, or latches to keep the tool secure while moving.

Before the advent of quick-attach tools, the tools were directly and permanently fixed to the loader arms using pivot pins that were held in place by various methods including snap rings, roll pins, and cap screws. The lower set of pins secured the tool to the loader arms and served as a pivot for tool movement. The upper set of pins attached

the mechanical actuators (usually hydraulic cylinders) to the upper end of the tool. The hydraulic cylinders served to position the tool as it pivoted around the lower pin joint as shown in Figure 3.

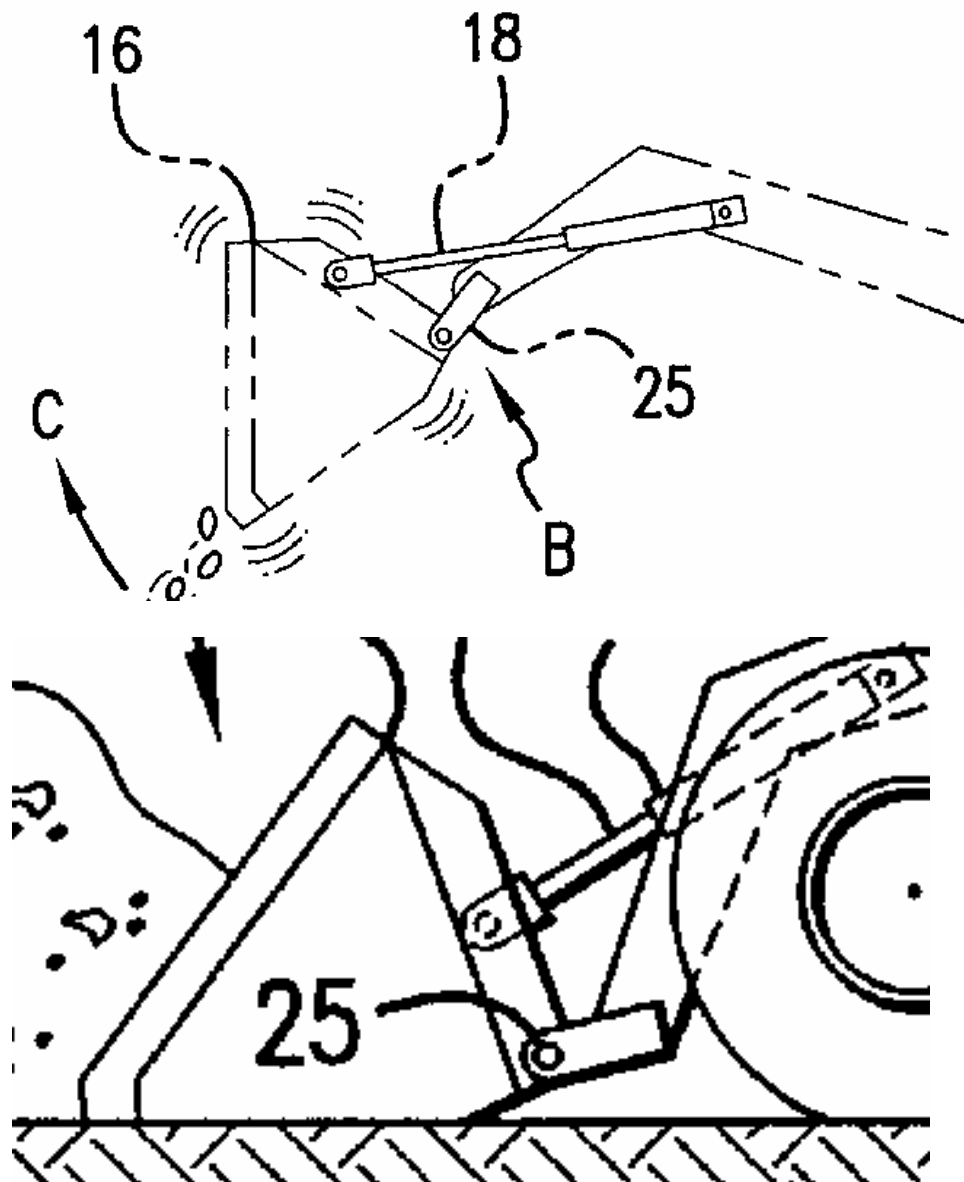


Figure 3: Original Tool Attachment [16]



Many early models of quick attach equipment are a simple variation of the original tool mounting setup. They use the existing pins which connected the arms of the machine to the tool, with no changes to the tool [17]. The arms of the machine are fitted with an adaptor with the original attachment pins. A second set of pins is inserted into the tool as before. To attach the tool to the arms, the adaptor is hooked into the upper pair of the pins, and then rotates down to cradle the lower set of pins. A latch then secures the lower end of the tool. This design is a simple, effective approach that works well with loader buckets and pallet forks.

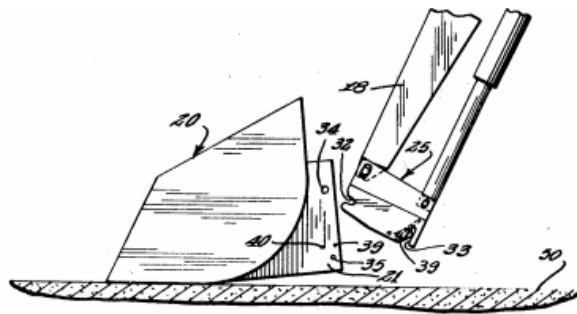


Figure 4: Patent Number 3,606,052 Dual [17]

Other types of attachment systems use various means of attaching the upper end of the implement, as in Figure 4, and lock pins to secure the lower end of the implement, shown in Figure 5 [18]. The lock pins are retractable for removing the implement, and are held in their locked positions by a spring. The pins are not positively held in the locked position. However, the pins only support a shear load, and do not experience any load that would unseat them from their locked position.

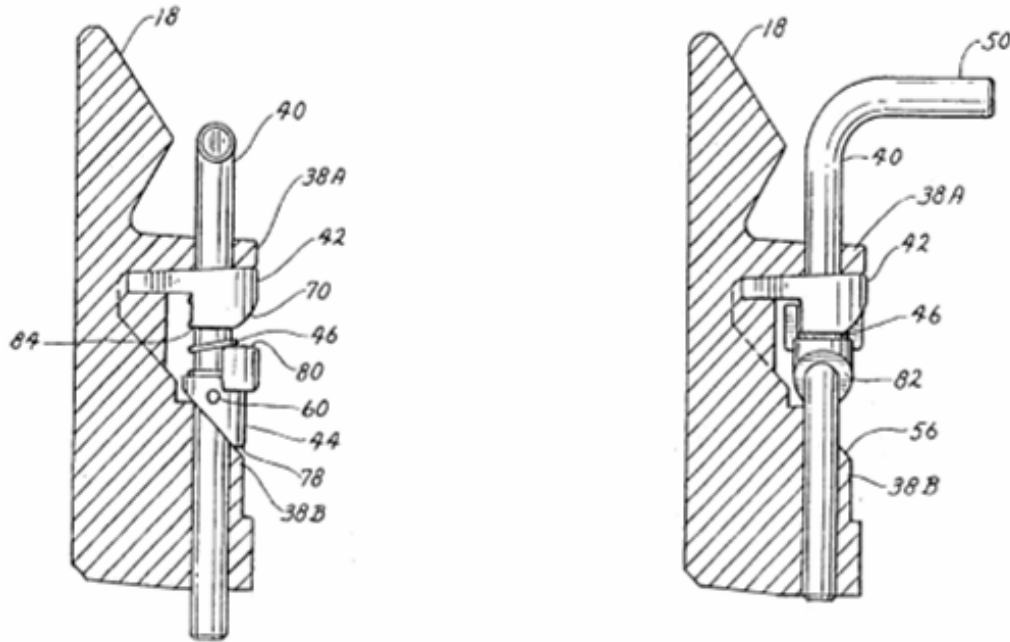


Figure 5: Patent Number 6,851,916 Toro [18]

Another type of attachment system also uses pins in the lower end, but the pins are pushed into their seats conjointly by a somewhat complex handle controlled mechanism. Positive stops are attached to the device that limit the motion of the handle from locked to unlocked. A torsion spring holds the mechanism in the locked position. This type of attachment system is shown in Figure 6 [19].

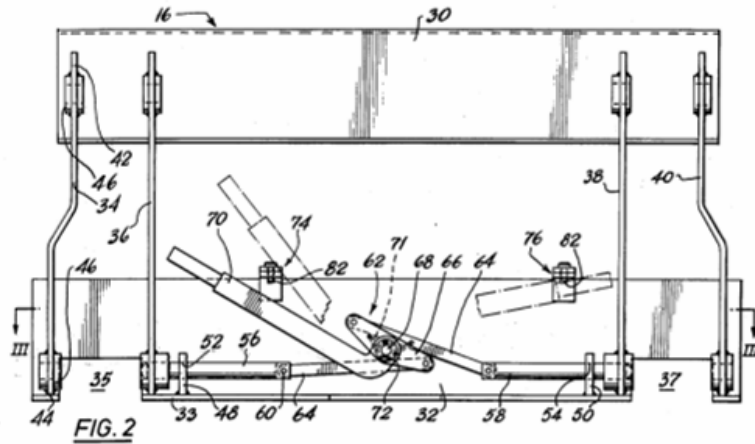


Figure 6: Patent Number 4,030,624 Massey Ferguson [19]

The most common and recent of these attachment devices is comprised of a lipped support at the upper end of the implement and angled locking surfaces at the lower end of the implement. The attachment bracket has a surface that supports the lip of the implement and locking mechanisms at the lower end. The locking mechanism has a pin with one end tapered that are controlled and held in place by a handle and a spring-loaded center link. The mechanism uses an over-the-center action to push the pin into its locked position and detent into that position. The spring loaded link holds the pin snugly into its locked position, and creates a detent that holds it in that position (Figure 7) [20].

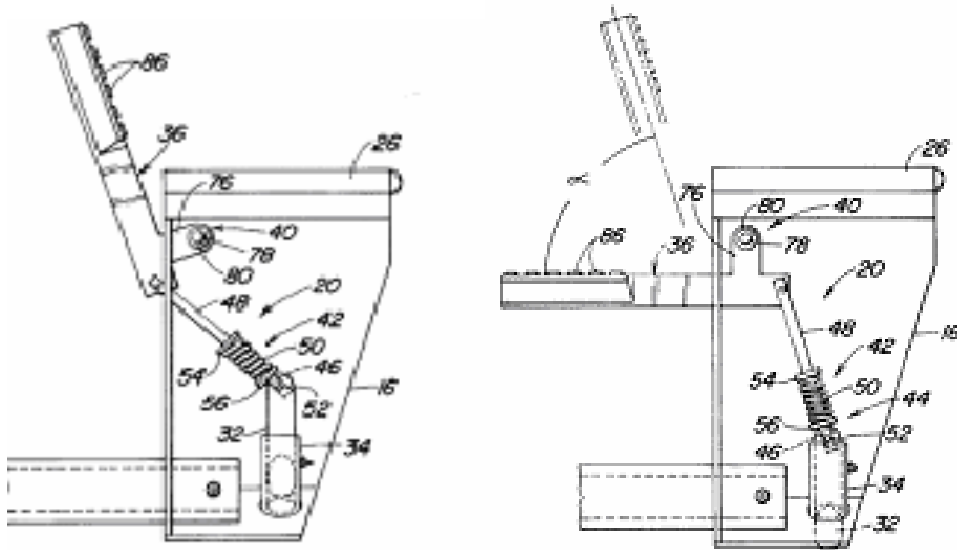


Figure 7: Patent Number 5,836,734 Deere [20]

The mechanism shown in Figure 7 is used widely across the industry in recent machines. The patent above is assigned to Deere and Company. Bobcat (Figure 8) [21] and CNH (Figure 9) [22] have patents of very similar attachment devices and these devices can be seen on many of their machines. These designs have proven to be reliable, easy to use systems for the attachment of implements to their respective machines.

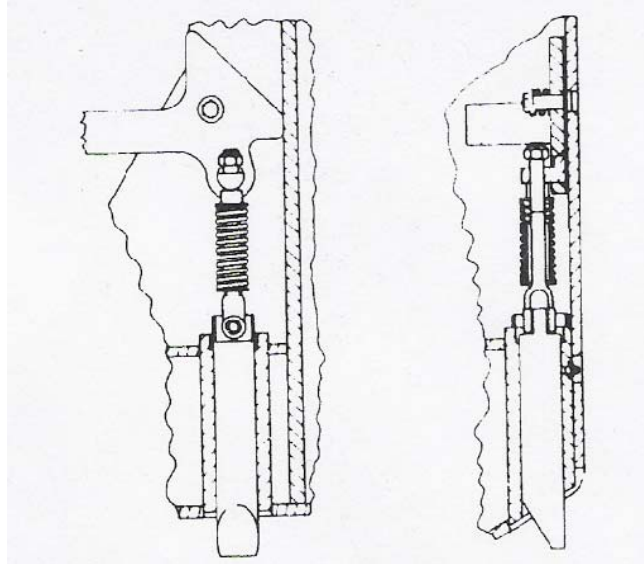


Figure 8: Bobcat Quick Attach [21]

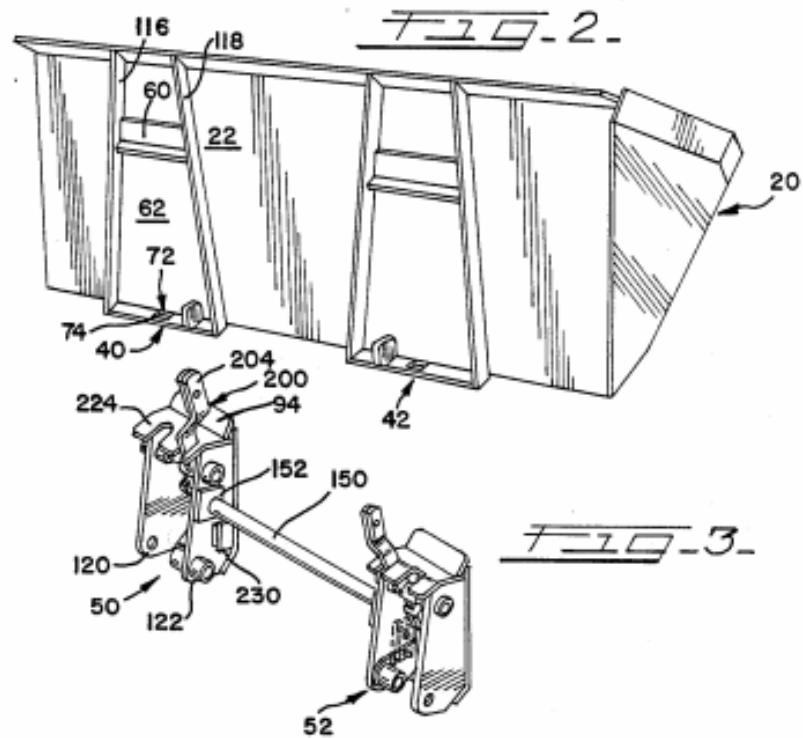


Figure 9: Patent Number 4,812,103 Case [22]

### Quick Attachment Review Summary

Reviewing previous designs of quick-attachment devices was the first step in designing a similar device for the Oculus sensor platform. The sensor platform is similar to the machines discussed in this review in that they consist of a set of load-supporting arms that carry and control a tool, or a sensor pod in this case. It is sought to have the pod easily detachable and re-attachable, as are the tools discussed here, while maintaining a safe and secure connection.

The design of the quick-release mechanism for the sensor platform will be somewhat similar to those discussed in the review. However, this design will have some major dissimilarity. The pod does not need to rotate independently of the arms, so the pin-pivot joints will not be necessary. The sensor pod will also be subject to different loading, vibration, and safety concerns than those machines, so the components of the new mechanism will be designed around its own loading criteria.

## 2.2 Finite Element Analysis Review

Finite Element Analysis (FEA) is a computational technique used to obtain approximate solutions of boundary value problems in engineering [23]. The key idea behind the finite element method is to discretize the solution domain into smaller, simpler domains called elements [23]. The problem then becomes many smaller, simpler problems with smaller, simpler solutions. The solutions are then assembled back together and checked for the “smoothness” of the solution. The process is iterated as many times as it takes to get the desired smoothness. Until the age of computers, this process was not practical, as an engineer may have to solve countless equations. Today, Finite Element Analysis is readily available as one of engineers’ most valuable tools. From Feragotti, “The Finite Element Method (FEM) is quite possibly the most important tool added to the mechanical design engineer’s toolbox in the last 20 years, and can be used to obtain more accurate design computations in complex situations” [24].

Traditionally, in order to develop a product, engineers would have to create a prototype through the use of hand calculations which are based from assumptions of the component’s behavior under design loading conditions. The prototype was then subjected to testing under the design conditions where flaws in the design would appear. Based on the nature of the design flaw the product would then be redesigned and tested again. This process would have to be repeated many times until a successful prototype was generated. With the introduction of FEA methods in the product development process, a more accurate portrayal of the component’s behavior under loading conditions can be examined. The use of FEA software also allows engineers to spend less time solving for the component reactions to various loads and to concentrate harder on the loading

conditions and the development of a more accurate operation loading environment. This enables engineers to develop a prototype which will require a fewer number of design iterations and allow for the component to reach the production phase much faster and at a lower cost. Studies have shown that through the use of computer aided design a time savings of 27% and a cost savings of 32% on average have occurred in product development and production [25]. Because of the availability of sophisticated commercial finite element software, the finite element method has become the preferred method of solution for many practical problems [23].

#### Finite Element Analysis Review Summary

The Finite Element Analysis Review was performed to generally explain the way the Finite Element Method works. Some components of the design of the quick-release mechanism are too complex to analyze using hand calculations, so FEA was used to calculate the stresses and displacements of those components. It was also used to illustrate how the stresses act on the components.



### **3.0 Quick-Release Design**

This section will cover the overall design of the quick-release mechanism and its various components. The overall geometry of the system and its components will be calculated, followed by a loading analysis of all the components and the mechanism. Redesign and reanalysis of the components will follow where necessary.

The proposed system is similar to those used on utility machines, as discussed above. It will allow easy mounting and dismounting of the pod from the arms by unlatching two handles. The device is shown in Figure 10. The exploded view is shown in Figure 11 and Table 1.

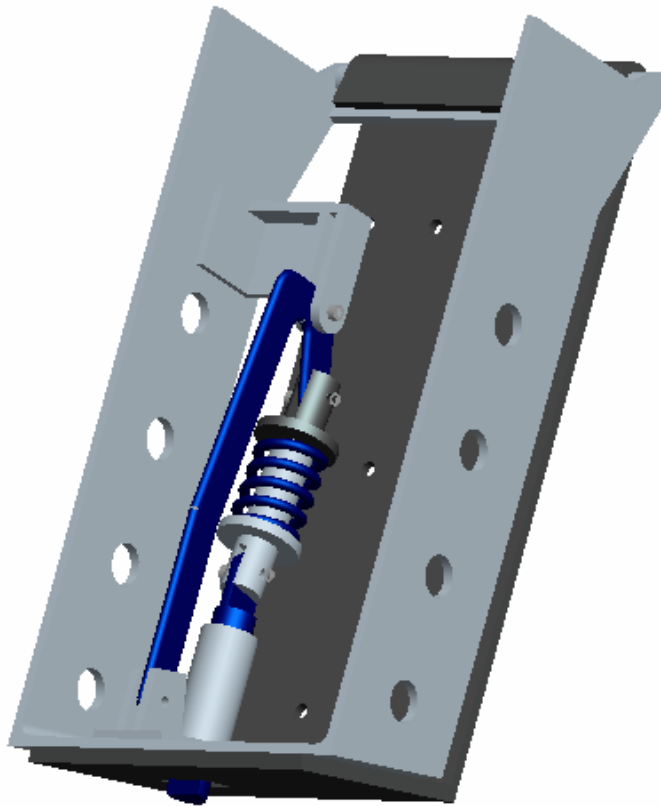


Figure 10: Quick Release System

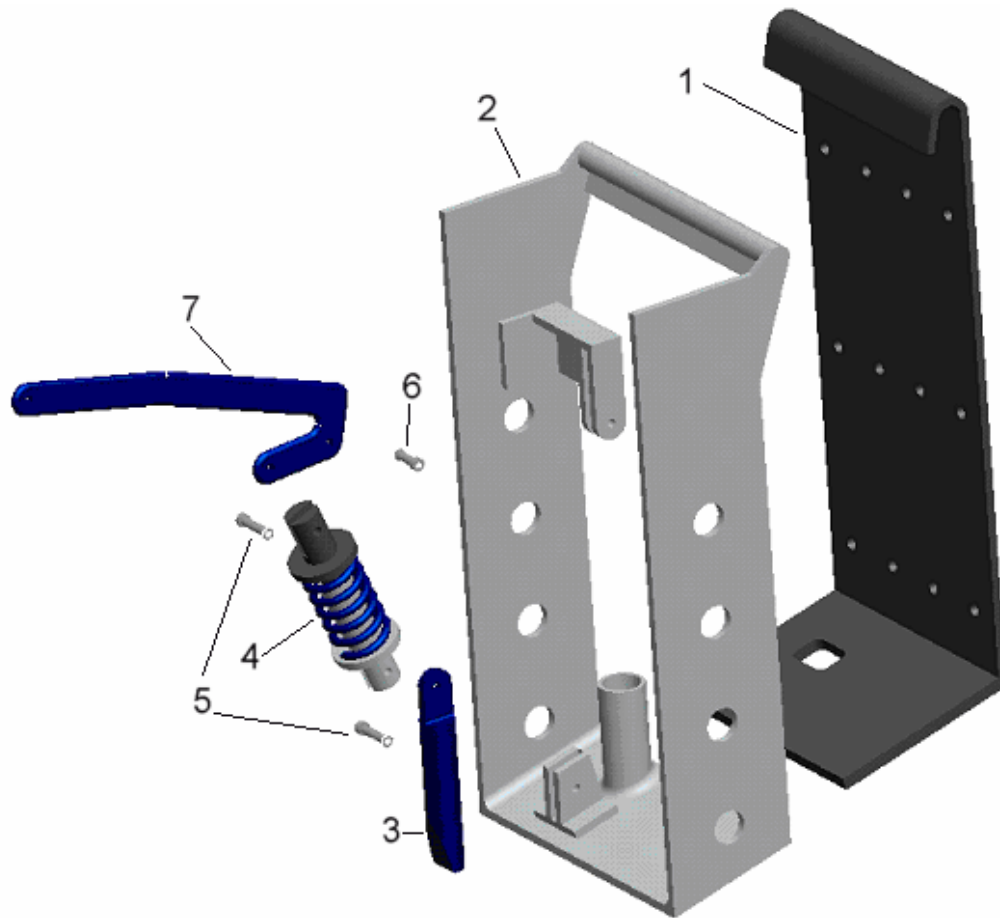


Figure 11: Exploded View of Components

Part Number	Description	Qty
1	Pod Attachment Bracket	1
2	Arm Frame	1
3	Lock Pin	1
4	Spring Link	1
5	Shoulder Bolt, 1/4" X 1"	2
6	Shoulder Bolt, 1/4" X 3/4"	1
7	Handle	1

Table 1: Component List

### Latching Mechanism

The latching mechanism is the apparatus that will serve to secure the pod to the arms, while allowing the capability to release the pod from the arms. The mechanism was designed using Pro/Engineer and AutoCAD drawings from original hand drawings. AutoCAD and hand drawings were developed to find the correct workable geometry of the mechanism. Using Pro/Engineer facilitated in component fitment, clearance, and analysis.

### Design Constraints and Requirements

The first condition was the space allowed for the components of the mechanism. All of the components must reside in the space between each set of arms and between the mounting flanges of the pod, shown in Figure 12. The mechanism must sit fully in the space between the arms and the pod flanges so that a sealed cover may be added in the future to seal the mechanism, the pod and its payload from the elements. Also, this area is used for routing the sensor power and data cables. Therefore the mechanism must not fill the entire available space between the pod surfaces and arms.

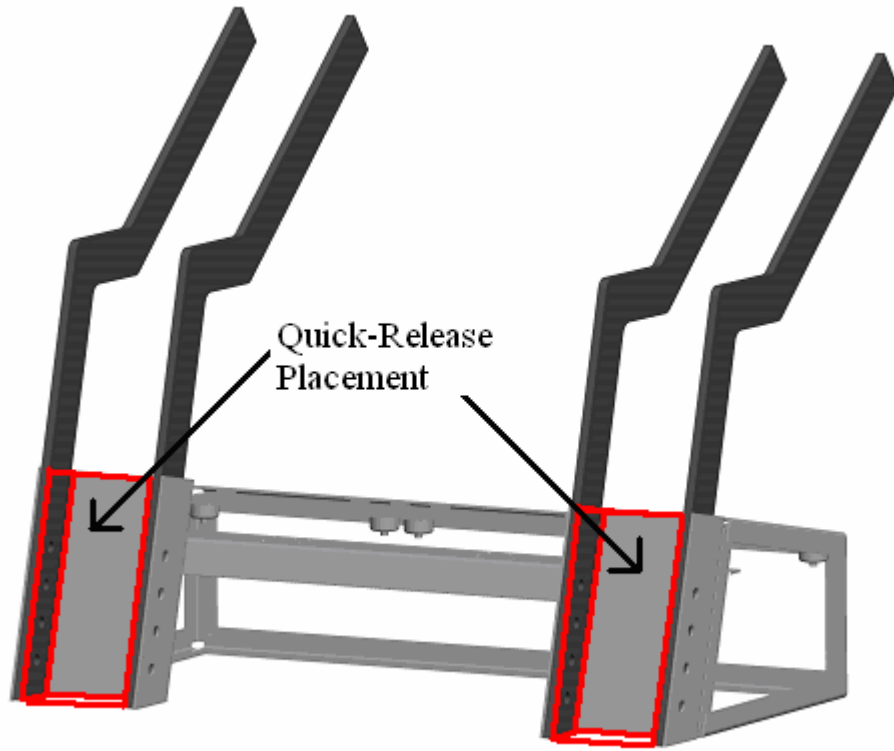


Figure 12: Space Allowed for Attachment Device

The space limitations were a key consideration in the design of the action of the mechanism. The pin must translate into the pod's latch member enough to ensure a positive latch, and must retract enough to release the pod. The motion of the pin determines the motion of the spring link, and the spring link determines the rotation of the handle. The rotation distance of the handle must be adequate to retract the pin, and must be large enough to easily load the spring.

The loads on the components were the other major design consideration. The pins must be large and strong enough to handle the loads that will act on them during mid-deployment, since they will carry their largest load at this position. The spring link must

have enough potential so that it will load the pin with enough force to react to loads that will try to force the pin out of its locked position.

The mechanism design chosen closely follows that of the newer front end loader / skid steer loader designs shown in Figures 7, 8, and 9. The upper end of the pod will “hang” on a rail, and the quick-release mechanism will latch the lower end into place. The mechanism consists of a lock pin, a spring link, and a handle. These components are connected with ¼ inch shank shoulder bolts and locknuts. The mechanism uses an over the center action to load the spring, which will keep the pin in place during flight. The spring will also allow for a small amount of wear in the pin contact area. The mechanism also causes a positive locking effect – in the case of spring failure, the quick-release mechanism will not allow the pod to become loose from the arms because of the geometry of the mechanism. When the handle is in the latched position, the spring link will not be able to shorten enough to allow the lock pin to retract from the pod. An illustration of the mechanism is shown in Figure 13.

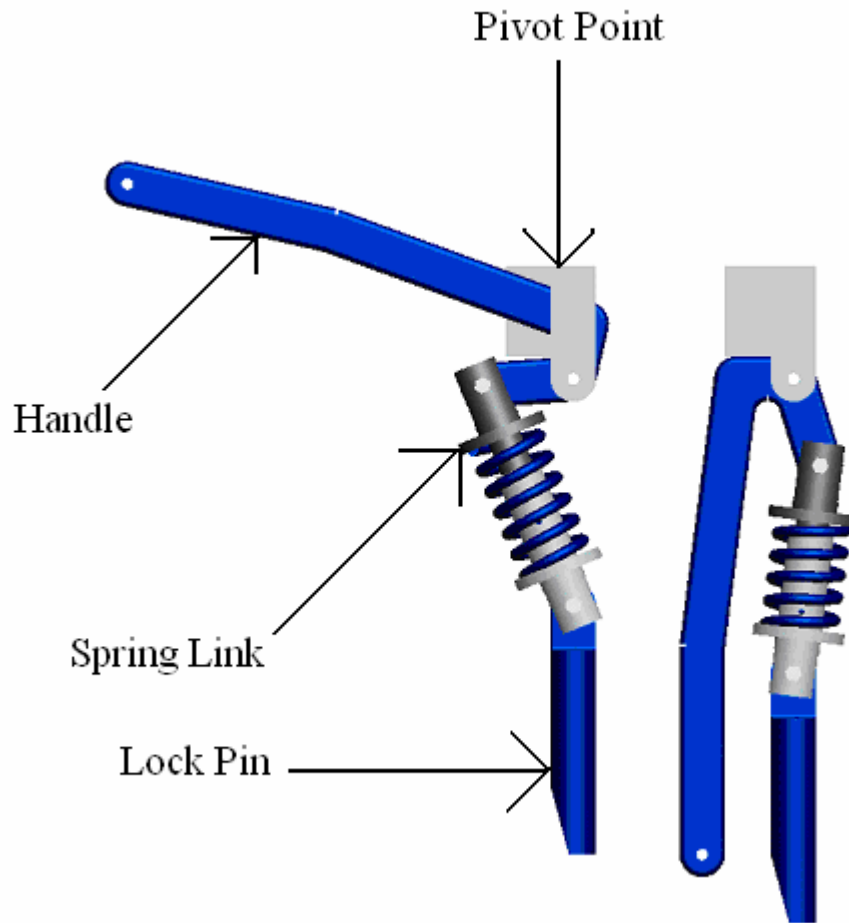


Figure 13: Comparison of Unlocked/Locked Positions

The mechanism also incorporates a secondary catch that will hold the handle in the latched position to serve as a backup in the case of spring failure. This secondary catch will also allow the pod to be locked to the arms by using a locking hitch pin. This “lock-out” will prevent removal of the pod, such as during maintenance, when in the stowed position, or in instances where the pod and its payload must be managed by a certified individual.

Two latching mechanisms will be used to attach the pod to the arms. They will reside in the areas shown in Figure 12. The pod and arms connected with the attachment device are shown in Figure 14.



Figure 14: Pod and Arms with Quick Attach Locked

The geometry of the mechanism was the first step in the design. The motion of the mechanism is like that of a slider-crank mechanism, with the connecting link being variable. The mechanism is of the 4-bar type, including the ground link, lock pin, spring link, and handle, as illustrated in Figure 15. This 4-bar mechanism allows one degree of freedom, which is the translation of the pin from the latched to the unlatched position. The geometry of the mechanism also amplifies the force input from the handle through the spring link to the pin, giving a high mechanical advantage. The mechanical

advantage will be discussed in the analysis section of this thesis. A simple diagram of the motion of the mechanism is shown in Figure 16.

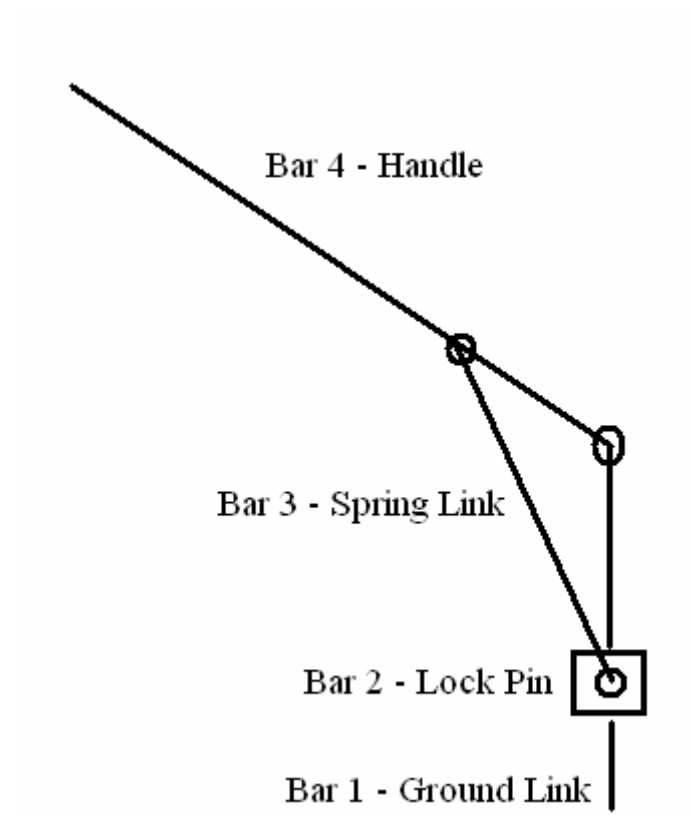


Figure 15: Diagram of 4-bar Slider-Crank Mechanism



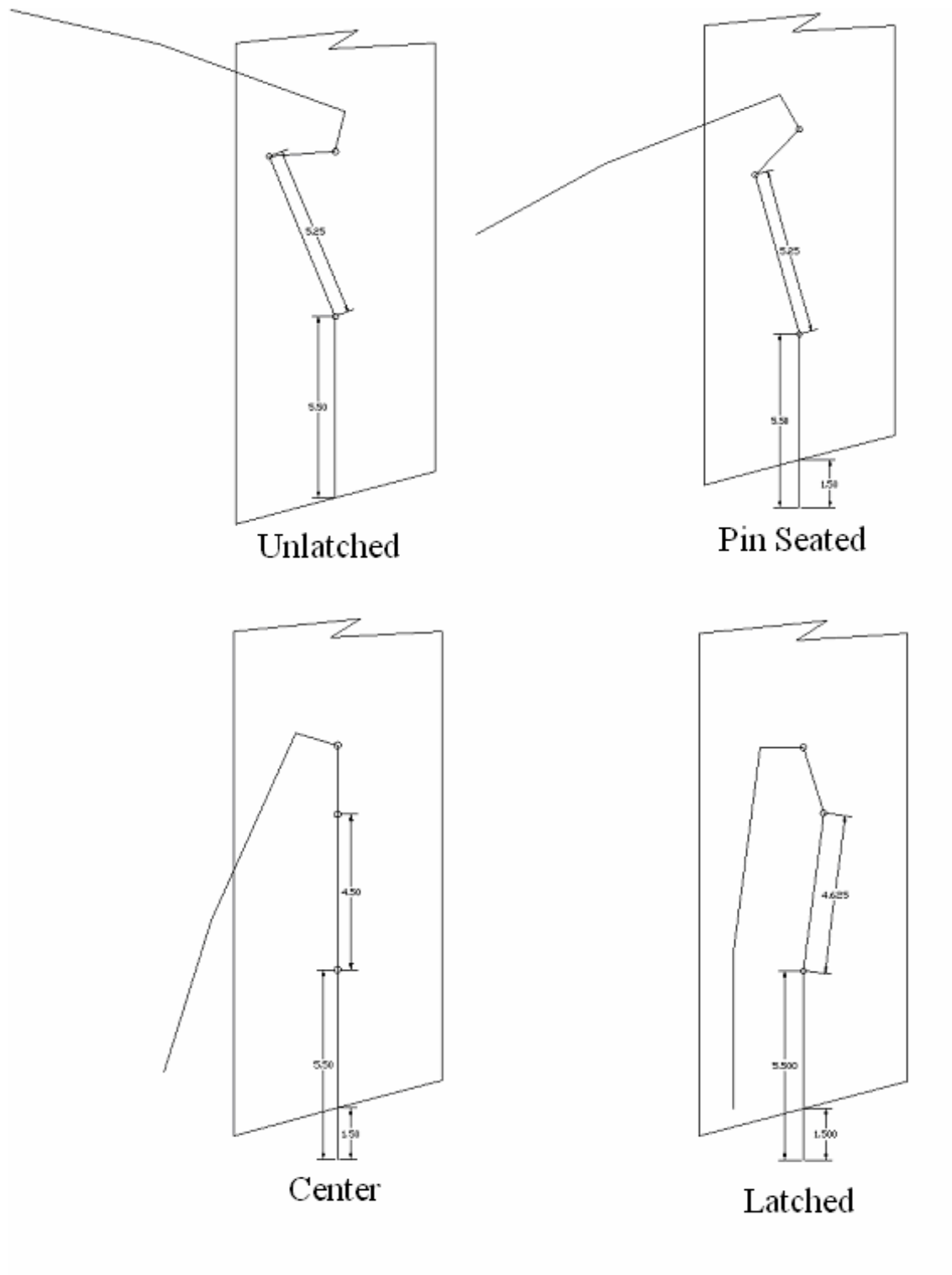


Figure 16: Geometry of Mechanism

### Lock Pin Design

The lock pins (Figure 11) are used to secure the lower end of the pod to the arm frame. The pins are held in place by the spring link on the latching mechanism, as shown in Figure 13. The pins are made from one inch diameter 4130 aircraft grade round bar steel. They are tapered at the contact surface to ensure a secure fit and to reduce point forces and high stresses. The taper angle is matched to that of the rear surface of the pod, so that forward loading on the pin will be perpendicular to the tapered surface. The connection end of the pin is machined to  $\frac{1}{4}$  inch thick to fit the spring-links and rounded to allow clearance for mechanism rotation.

The lock pins will be tapered so that it will meet its mating surface perpendicularly. To achieve this, the pin's taper is oriented 15 degrees from vertical (in reference to the arms), since the mating surface is 15 degrees from horizontal (in reference to the pod). In tapering the pin, the height of the taper comes to be 1.866 inches from the lower end of the pin. The pin is to be seated at its mating surface at the midpoint of the tapered surface, or 0.933 inches from the end of the pin. The mating surface will be 0.375 inches, so the pin must travel 1.308 ( $0.933+0.375$ ) inches vertically. In order to have positive clearance, a translation distance of 1.5 inches was chosen.

### Spring Link Design

The spring link (Figure 11) connects the handle to the lock pin. It consists of a male and a female end that slide axially and a compression spring that forces the pin to its greatest length. The ends are held together by a spring pin (Figure 17). The spring pin

chosen is a heavy duty coiled spring pin, .125 inches in diameter and 1 inch long, with a max load rating of 2000 pounds.



Figure 17: Spring Pin

When in the locked position, the spring is loaded and pushes the lock pin into place. At this position, the spring link is compressed to near its shortest length and the case of spring failure, obstruction, or high loads will not allow the lock pin to retract from its locked position. This spring link creates a toggle effect, since the mechanism “toggles” between the latched and unlatched positions.

The spring-loaded connecting link is variable in length. The spring is a high-load compression spring made of chrome-silicon steel and has a spring rate of 1000 pounds per inch. The spring is 2.5 inches long, and its wire size is .195” x .468.” When the mechanism is in the unlatched position, the spring will force the link to its greatest length, 5.25 inches, and the link will act only as a connecting link. As the mechanism is moved to the center position, the spring will compress 0.75 inches, and the link will measure 4.5 inches, as illustrated in Figure 16, 18, and 19. When in the over-center, latched position, the spring will remain compressed 0.625 inches. The lengths of the spring link were chosen to be the shortest possible, when using a 3 inch spring with a

0.75 inch loaded displacement. The variation in the length of the spring link is illustrated in Figure 19.

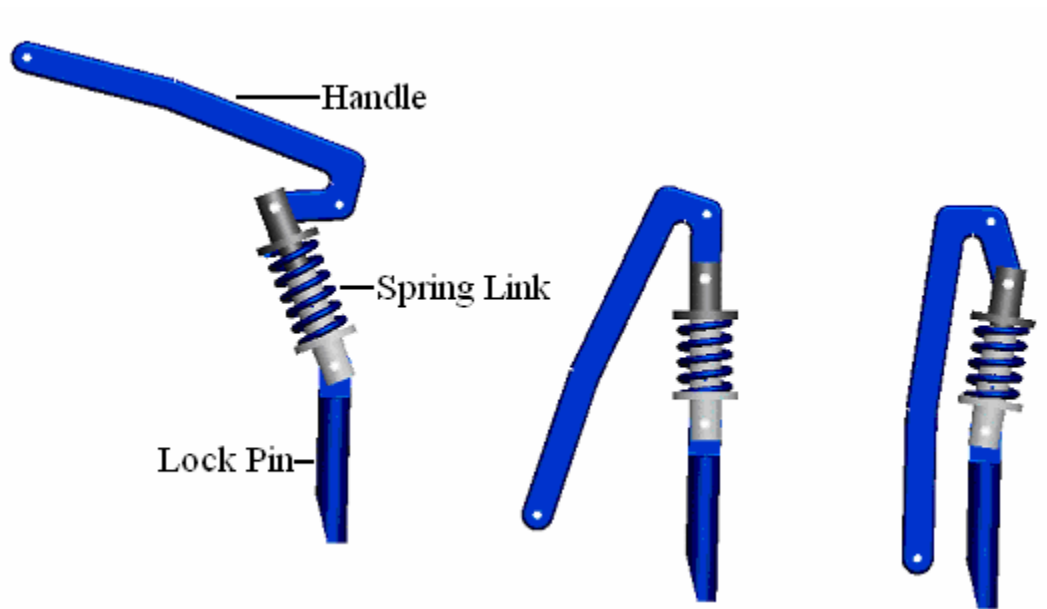


Figure 18: Mechanism in the Unlocked, Center, and Locked Positions

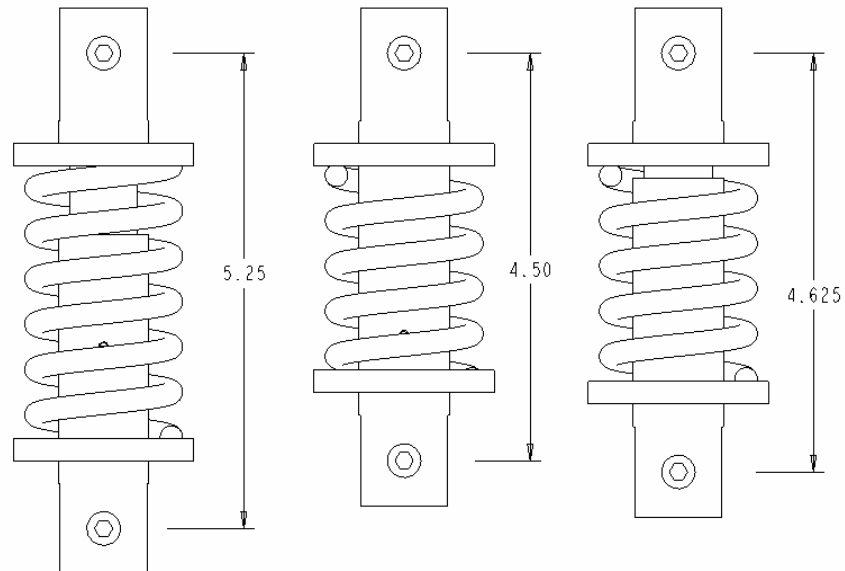


Figure 19: Spring-Loaded Link in the Unlocked, Center, and Locked Positions

### Handle Design

The handle (Figure 11) is the component that will allow the user to latch the device. The handle will also be used to “lock-out” the device.

The handle must be long enough to make the mechanism easy to latch and release, but must fit within the allotted area. The handle is made of ¼ inch 4130 steel flat stock. The hooked end of the handle has two holes, one that will serve as the pivot point and another that will be the connection point for the “crank” component of the slider-crank mechanism.

### Mechanism Design Summary

The geometry of the mechanism was calculated using the space-limitation constraints and the pin translation requirements. The spring link was designed with the smallest possible dimensions that would still allow the deflection needed to load the spring and the overall length needed to retract the pin from its locked position. The angle of rotation of the handle and the translation distance of the pin are shown in Figure 20.

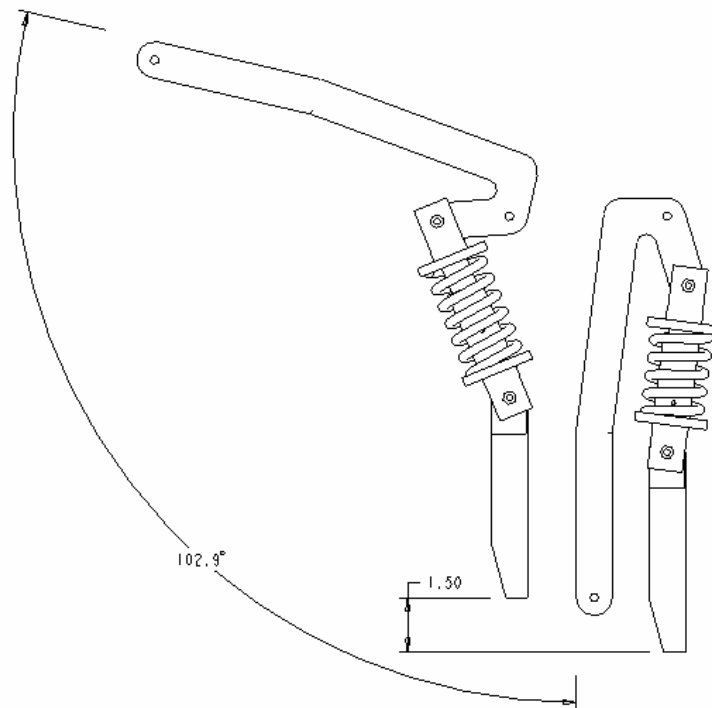


Figure 20: Angle of Rotation of Handle and Distance of Translation of Pin

### Pod Attachment Bracket Design

The pod attachment bracket (Figure 11) is the component that will secure the pod to the attachment device. The bracket will be designed to be as simple as possible while being rigid enough to support the weight of the pod.

The pod currently in use is built by APX Enclosures, Inc. of Mercersburg, PA. It is built from 5052-H32 aluminum and is designed to carry up to 1000 pounds of sensor payload. Part of the design of the quick attach system is to have the fewest modifications to the pod as possible, so that structural integrity of the pod is not compromised and so that many pods may be set up to fit the quick-attach system at the lowest cost.

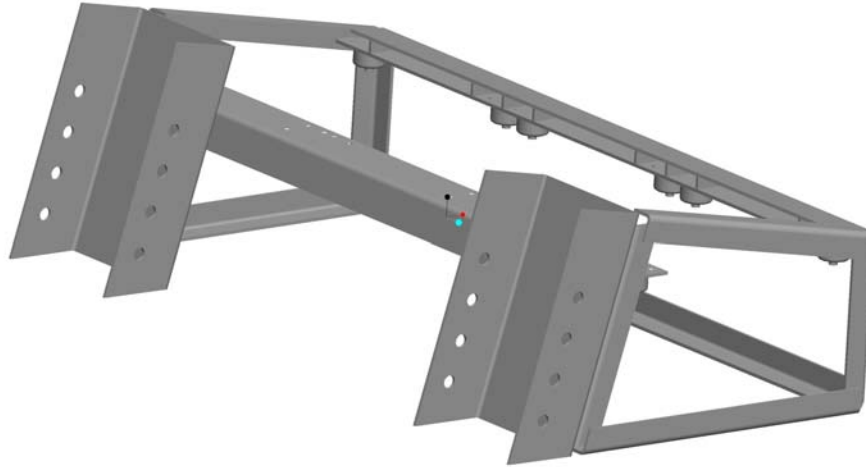


Figure 21: Sensor Pod Frame

The pod frame without the outer skins is shown in Figure 21 with previous attachment points. The pod was bolted to the arms using 1 inch bolts through the holes in the mounting flanges.

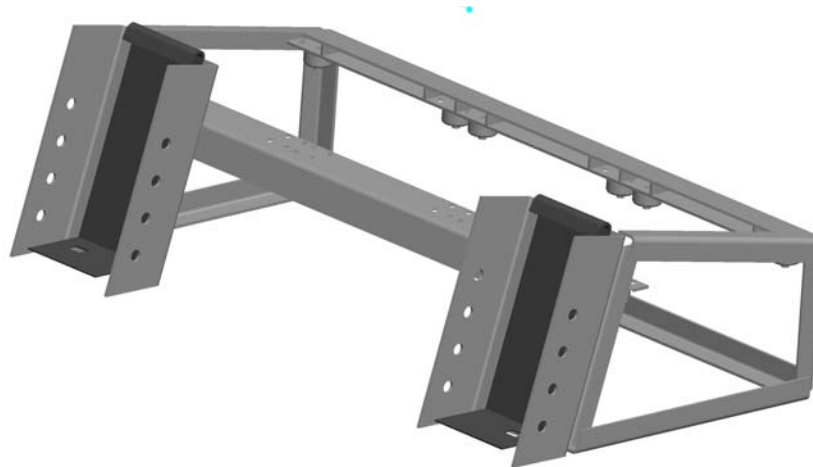


Figure 22: Sensor Pod Frame with Attachment Brackets

The pod attachment brackets will be the only addition to the pod as shown in Figure 22. These brackets are made from 4130 aircraft grade steel. This steel was

chosen since it meets military specifications. The bracket has a long hook that will hang over its mating surface on the arms. The lower, angled plate will rest against its mating surface attached to the arms. The lock pin will seat into the square hole in this bracket (Figure 23), which will lock the pod into place.

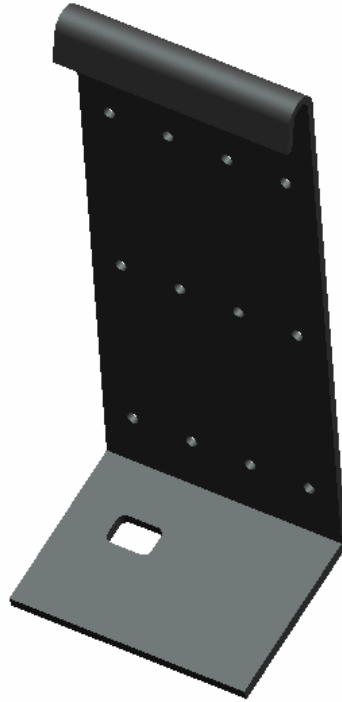


Figure 23: Pod Attachment Bracket

The pod attachment brackets will be fixed to the pod using military grade bolts and locknuts. Two attachment brackets will be used, as shown in Figure 22.

### Frame Design

The arm attachment frame (Figure 11) will be the main component of the attachment device. It will be fixed permanently to the arms. The frame will carry the latching mechanism and will support the load of the pod.



The frame will attach between each pair of arms (Figure 24). It is made of 4130 aircraft grade steel flat stock and tube. It consists of two straps that will be secured to the arms and a round bar at the upper end which will support the weight of the pod in the deployed position. The lower surface of the frame is situated at an angle relative to the arms that will position it level with the aircraft. It will also mate firmly with the lower surface of the pod attachment bracket and will carry the majority of the load when the pod is in the stowed position.

The frame holds the locking mechanism in place. The lower surface of the frame includes a steel tube which will support the lock pin. The pin will slide in this tube when it translates from the locked to the unlocked position. The handle pivot support is also attached to the frame. The pivot support is the component that holds the handle in place and allows rotation of the handle.

The only modification to the arms will be to countersink the existing holes to accept countersunk, socket head cap screws. This will allow clearance for the pod mounting flanges. The flanges will be kept on future pod designs for alignment purposes and lateral rigidity.

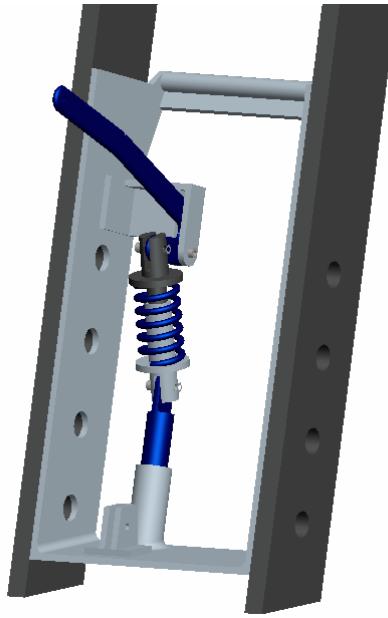


Figure 24: Arm, Frame, and Latch Mechanism Assembly

### Design Summary

The geometry of the quick attach mechanism was first determined through the use of AutoCAD drawings shown in Figure 16. The design was then created in three dimensional models in Pro/Engineer and incorporated into the models of the pod, arms, and sensor pallet to check for clearance issues and part fitment. The three dimensional model was then assembled using Pro/Engineer Mechanism to check mechanism motion and clearances.

#### **4.0 Component Analysis**

The components were analyzed using hand calculations (4.1, 4.2, and 4.3), spreadsheets (Appendix A), and Finite Element Analysis in Pro/Mechanica (Appendix B). All of the components were analyzed in the deployed, mid-deployment, and stowed positions with 1000 pounds of sensor load to simulate varying loading situations. The maximum values of loading were based upon MIL-HDBK-1791 load criteria of 4.5 G down [26]. The value of 4.5 G is used throughout this analysis. A safety factor of 1.5 must be met with each structural component. Also, a modal analysis of the components was performed using Pro Mechanica to check the natural frequencies. Since the platform will not continuously operate under the maximum load criteria (4.5 G), and the design incorporates a safety factor of 1.5, a fatigue analysis is not necessary. The quick-release mechanism will cycle at loads significantly lower than those in the stress analysis.

#### **Mechanism Analysis**

The analysis on the mechanism as a whole was to ensure that the lock pin stays seated in its locked position. It also ensures that the spring link will keep pressure on the handle to keep it in the locked position while still allowing easy unlatching of the mechanism.

The first analysis is of the force of the pod on the pin in the direction that would try to force the pin into an unlatched condition. The position analyzed was mid-deployment since this is the position where the pin will carry the highest load and the force on it will be in the downward direction. In all other positions the load will be carried by some other component of the system. The pin is situated at 75 degrees from

vertical when in the mid-deployment position as shown in Figure 25. The pin will support one-half of the total weight of the sensor pod, or 500 pounds. At 4.5 G, the pin will support a force of 2250 pounds. The axial force on the pin was found as follows:

$$F_A = \cos \Theta * F_D, \quad \mathbf{4.1}$$

where

$F_A$  = Axial force on the pin,

$\Theta$  = angle between the pin and the load, and

$F_D$  = downward force from the pod's weight.

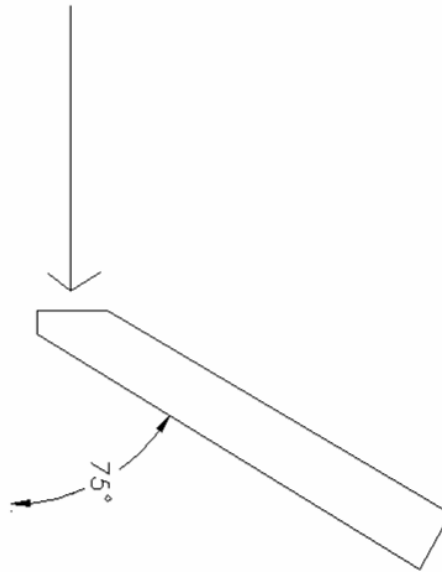


Figure 25: Loading on Pin at Mid-Deployment

The axial force on the pin was found to be 582.34 pounds. Consequently, the spring link will need to be strong enough to react to this loading.

The spring link in the locked position is situated at 7.27 degrees with respect to the lock pin, as shown in Figure 20. The spring force needed was found as follows:

$$F_s = \frac{F_A}{\cos \Theta}, \quad 4.2$$

where

$F_s$  = force of the spring link, and

$\Theta$  = angle of spring link with respect to the lock pin.

The spring force needed from the spring link was found to be 587.06 pounds. The spring rate needed was then found using:

$$k = \frac{F_s}{x}, \quad 4.3$$

where

$k$  = spring rate and

$x$  = deflection of the spring.

The deflection of the spring in the locked position due to the geometric design of the mechanism is 0.625 inches, as discussed in the design section and illustrated in Figure 16. The spring rate  $k$  needed was 939.30 pounds per inch. This is satisfactory since a 1000 pound per inch spring was chosen.

The next check was on the mechanical advantage produced by the mechanism and of the load on the handle and the user-force needed to unlatch the mechanism. This was checked using Microsoft Excel to calculate the force on the handle at all positions between unlatched and latched in one degree increments. These values were then used to

find the force caused by the spring onto the handle and the lock pin. The spreadsheet can be found in Appendix A. Figure 26 illustrates the force needed by the user on the handle and the respective force on the pin from 0 to 102.9 degrees of rotation of the handle.

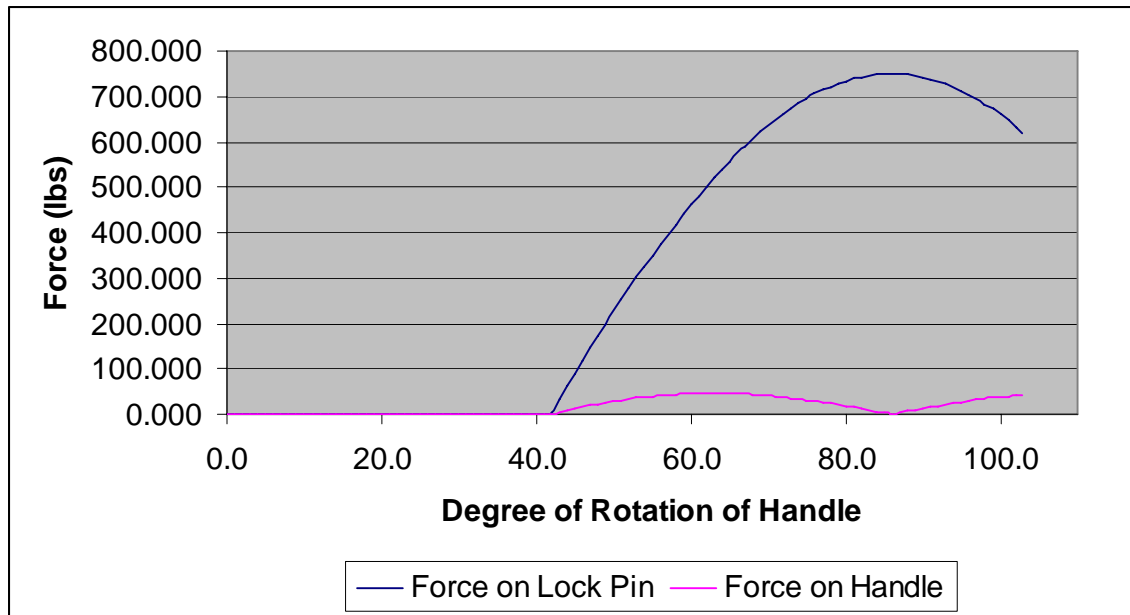


Figure 26: Mechanical Advantage Force Comparison

The force needed from the user to unlatch the mechanism was found to be about 43 pounds when a spring with a spring rate  $k$  of 1000 pounds per inch and a 12 inch handle are used. The force holding the pin in the latched position is 620 pounds. This value is satisfactory since it exceeds the force value of 587.06 pounds, found previously.

#### Pod Attachment Bracket Stress Analysis

The pod attachment bracket was analyzed in the deployed position, the stowed position, and the mid-deployment position using 4.5 G in the downward direction. The three analysis positions were chosen because each position causes a high-loading effect

on a different area of the component. The constraints were applied at the mounting locations (bolt holes) and the loads were applied according to the component's position.

In the first analysis, the attachment bracket was situated as it will be in the deployed position. The load was applied to the inside of the upper curved surface, since this area will support the entire load of the pod when the system is in the deployed position. The load was applied in the upward direction, the direction in which it will act on the component. The load applied was calculated by taking the total load of the pod, 1000 pounds, dividing by 2 since there are two pod attachments, and multiplying by 4.5 G, the maximum worst-case loading scenario. The loading of the pod attachment bracket in the deployed position is shown in Figure 27. The results of this analysis are listed in Table 2 and illustrated in Appendix B.

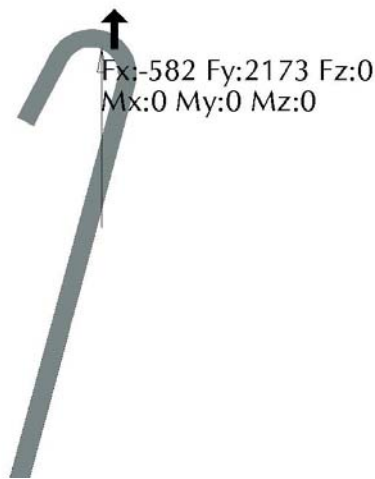


Figure 27: Load Applied to Pod Attachment Bracket in the Deployed Position

The second analysis on the pod bracket was done in the mid-deployment position. In this position, the forces will act on the hooked surface and at the lock pin surface of the square hole. The forces were applied in the vertical direction. The analysis is

illustrated in Figure 28. The results of this analysis are listed in Table 2 and illustrated in Appendix B.

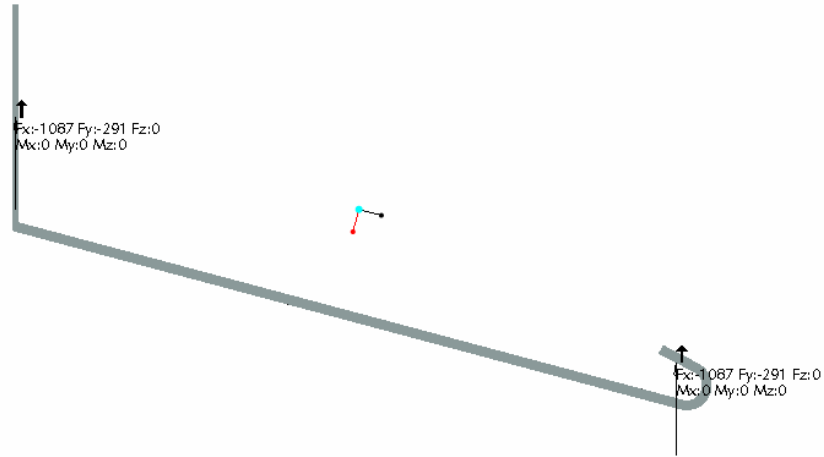


Figure 28: Load Applied to the Pod Attachment Bracket in the Mid-Deployment Position

The third analysis on the pod attachment bracket was in the stowed position. The forces were applied to the bracket's lower flanged surface, in the vertical direction (Figure 29). The results of this analysis are listed in Table 2 and illustrated in Appendix B.



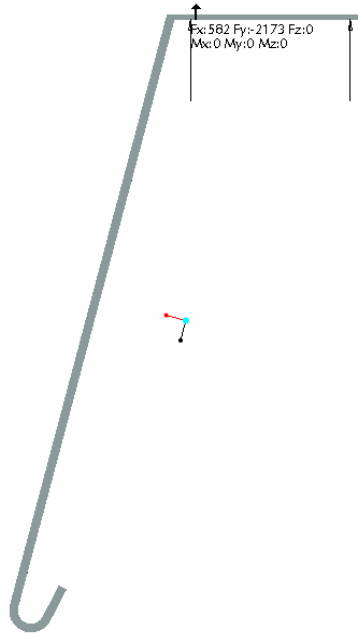


Figure 29: Load Applied to the Pod Attachment Bracket in the Stowed Position

### Arm Frame Stress Analysis

The arm frame was analyzed in the same manner as the pod attachment bracket. The frame was situated in all three positions with the loads applied respectively. The constraints were applied to the bolt holes of the component.

The first analysis was in the deployed position. The load was applied in the downward position on the upper bar, which will carry the entire load of the pod in this position. The loading is illustrated in Figure 30. The results of this analysis are listed in Table 2 and illustrated in Appendix B.

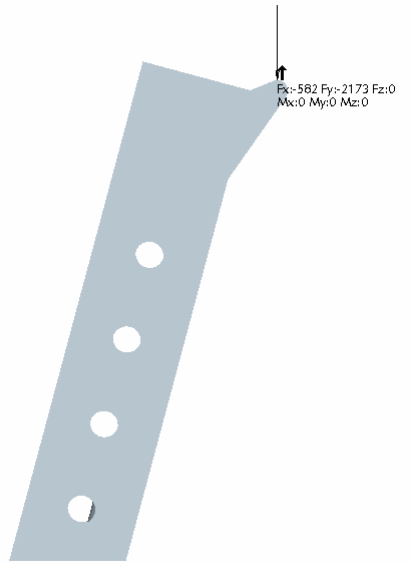


Figure 30: Load Applied to the Arm Frame in the Deployed Position

The second analysis on the arm frame was in the mid-deployment position. The frame was situated in that position and the loads were applied to the upper support bar and the lock pin surface in a downward direction. These areas will carry the load of the pod in this position. The loading is shown in Figure 31. The results of this analysis are listed in Table 2 and illustrated in Appendix B.

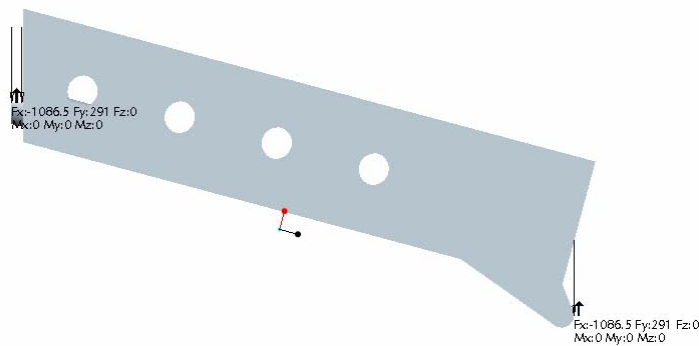


Figure 31: Load Applied to the Arm Frame in the Mid-Deployment Position

The third analysis on the arm frame was done for the stowed position. The load was applied to the lower surface as shown in Figure 32. The lower surface will carry the entire load of the pod when in this position. The results of this analysis are listed in Table 2 and illustrated in Appendix B.

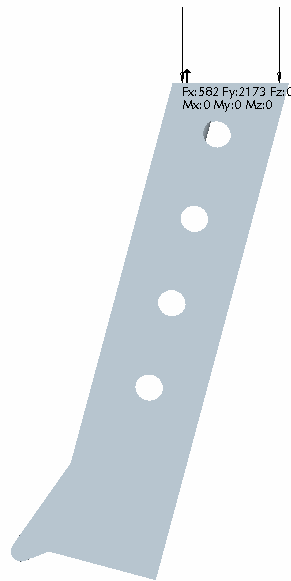


Figure 32: Load Applied to the Arm Frame in the Stowed Position

Another concern will be the bearing stress on the pin-constraining sleeve on the arm frame. The bearing area is 0.375 square inches. When loaded with the 500 pounds x 4.5G, the bearing stress is only 6000 psi, which is far below the yield stress of the material. The safety factor for this area comes to be about 9.

#### Lock Pin Stress Analysis

The lock pin was analyzed only at the mid-deployment position. This was the only analysis, since it will carry the highest load in this position. At all other positions,

the load will be shared by other components of the device. The downward load of 2250 pounds will not act on the pin in the stowed or deployed positions, and will act most on the pin in this position.

The pin was loaded across the tapered surface where it will meet the pod attachment bracket (Figure 33). It was constrained as it is held in place by the arm frame and latching mechanism. The results of this analysis are listed in Table 2 and illustrated in Appendix B.

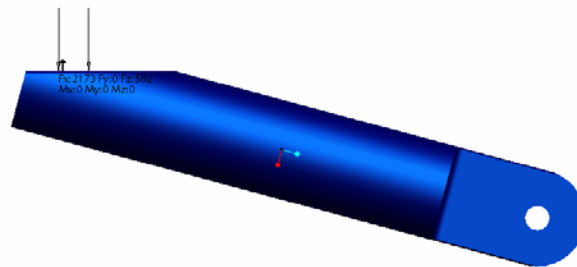


Figure 33: Load Applied to the Lock Pin in the Mid-Deployment Position

### Spring Link Stress Analysis

The spring link was analyzed using the highest forces that will act on the link, found using equation 4.2. The analysis was done on each component of the spring link individually, assuming that the spring has failed.

The first analysis was on the female component of the spring link. The load was applied to the outer surface of the connection (Figure 34). The pin was constrained on the inner mating surface in two directions and on the connection point. The results of this analysis are listed in Table 2 and illustrated in Appendix B.

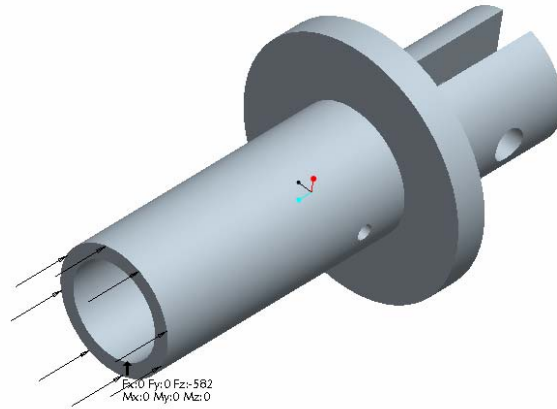


Figure 34: Load Applied to the Female Component of the Spring Link in the Latched Position

The second analysis was on the male component of the spring link. The load was applied to the end of the mating surface (Figure 35). The pin was constrained on the outer mating surface in two directions and on the connection point. The results of this analysis are listed in Table 2 and illustrated in Appendix B.

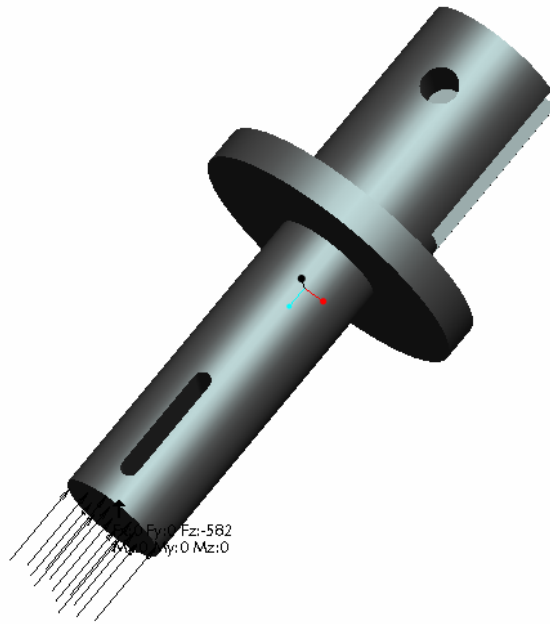


Figure 35: Load Applied to the Male Component of the Spring Link in the Latched Position

The spring pin that holds the spring link halves together has a maximum load capacity of 2000 pounds. The maximum force on the spring pin is 750 pounds, so the safety factor is  $2000/750 = 2.667$ .

#### Handle Stress Analysis

The handle will was analyzed using the force that will react to the force from the spring link found using equation 4.2. The force was applied in the direction parallel to the spring link (Figure 36). The handle was constrained at the pivot pin hole and at the secondary lockout hole at the end of the handle. The results of this analysis are listed in Table 2 and illustrated in Appendix B.

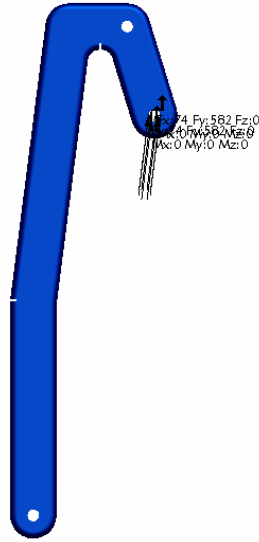


Figure 36: Load Applied to the Handle in the Latched Position

#### Shoulder Bolt Stress Analysis

The shoulder bolts cause two different stresses on the components' connection points. The first stress is the bearing stress of the shoulder bolt on the hole of the component and was calculated using the following equation:

$$\sigma = \frac{F_b}{A}, \quad 4.4$$

where

$F_b$  = force applied to each bolt,

and

$$A = td, \quad 4.5$$

where

$t$  = wall thickness of component, and

$d$  = bolt diameter.

The second stress generated on the bolt hole is that of a shear stress which acts to tear the bolt out of the arm (tear-out stress). This stress was calculated as follows:

$$\tau = \frac{F_b}{A}, \quad 4.6$$

where

$F_b$  = force applied to each bolt,

and

$$A = 2tw, \quad 4.7$$

where

$t$  = wall thickness of component, and

$w$  = distance from the center of the bolt hole to the edge of the component.

The shear stress acting on the shoulder bolt was also calculated, using

$$\tau = \frac{F_b}{A}, \quad 4.8$$

where

$F_b$  = force applied to each bolt,

and

$$A = 2\pi r^2 \quad 4.9$$

where

$r$  = radius of shoulder bolt.

The results of the shoulder bolt analysis are shown in Table 3.



### Stress Analysis Results

The analysis showed that all of the parts meet or exceed the strength needed. All of the parts have a safety factor greater than or equal to 1.5 when they are subject to a fully loaded pod at 1000 pounds and 4.5 G. All stresses found in the parts were well below the yield stress of the material used. All displacements found were very small and will not affect the positioning of the pod. The components' maximum von Mises stress values, yield stresses, and safety factors are shown in Table 1. The illustrated results of the Finite Element Analysis can be found in Appendix B of this thesis. The FEA results include the von Mises Stress values and locations and the displacement values and locations.

Component Description	Pod Position	von Mises Stress (psi)	Yield Stress (psi)	Safety Factor
Pod Attachment Bracket	Deployed	13,310	52,000	3.91
Pod Attachment Bracket	Mid-Deployment	11,460	52,000	4.54
Pod Attachment Bracket	Stowed	26,640	52,000	1.95
Frame	Deployed	32,080	52,000	1.62
Frame	Mid-Deployment	33,630	52,000	1.55
Frame	Stowed	34,750	52,000	1.50
Lock Pin	Mid-Deployment	23,070	52,000	2.25
Spring Link Female Component	Any	5,135	52,000	10.13
Spring Link Male Component	Any	2,685	52,000	19.37
Handle	Any	30,650	52,000	1.70

Table 2: Component Stress Analysis Results

Component	Bearing Stress	Tearout Stress	Shear Stress	Tensile Yield Stress	Shear Yield Stress	Bearing Safety Factor	Shear Safety Factor
Lock Pin	12000	4000	N/A	52000	30000	4.33	7.50
Spring Link	6000	2000	N/A	52000	30000	8.67	15.00
Handle	12000	3000	N/A	52000	30000	4.33	10.00
Arm Brace	6000	3000	N/A	52000	30000	8.67	10.00
Shoulder Bolt	12000	N/A	7600	97000	56000	8.08	N/A

Table 3: Shoulder Bolt Stress Analysis Results

### Modal Analysis

During flight, the sensor platform will be subjected to vibrations produced by the aircraft. If the frequencies of these vibrations match the natural frequencies of any of the components, the components will reach resonance and the resulting cyclic stresses could cause structural failure.

The components were analyzed using a modal analysis in Pro Mechanica to find their natural frequencies and the respective modes. Modal analysis determines the fundamental vibration mode shapes and corresponding frequencies. This can be extremely complicated when analyzing a complex mechanical device, so each component was analyzed separately. The components were constrained in the analysis closely to the way they will be constrained in the system during flight.

The vibrations from the aircraft will be in the lower frequency range of 18 Hz, as found during an aerodynamic rake test [4]. The natural frequencies of the components need to be significantly higher so that they will not reach resonance.

### Modal Analysis Results

The results of the modal analysis are listed in Table 4. The natural frequency of each component is considerably greater than the excitation frequency produced by the aircraft, 18 Hz. The modal analysis shows that the components will not resonate due to the aircraft vibration, and thus will not fail structurally. It should be noted that the vibration analysis results are limited due to the constraints used. The spring effect of the actual constraints on each component may alter the actual results.

Modal Analysis			
Component	Natural Frequency (Hz)		
	Mode 1	Mode 2	Mode 3
Pod Bracket	517	994	1650
Arm Frame	190	426	544
Lock Pin	23700	48500	54900
Spring Link Lower	2400	3410	6890
Spring Link Upper	1870	2660	6070
Spring	119	120	179
Handle	408	1100	1600

Table 4: Modal Analysis Results

### Fatigue Analysis

As the arms of the sensor platform rotate from the stowed position to the deployed position, the stress on the pod attachment bracket, frame, and pin varies from zero to the components' maximum stress, depending on their position. As the quick-release mechanism is moved from the latched position to the unlatched position, the same happens to the handle and the spring link.

A result of this varied loading is potential failure from fatigue of the components. In order to ensure that fatigue will not cause failure of the components, a modified

Goodman analysis was performed for each component. A Goodman diagram was constructed for each component (Figures 37-41) using the stress values used in Table 5. The yield line connects the yield stress on the x-axis with the yield stress on the y-axis. The Goodman line connects the ultimate stress on the x-axis with the endurance stress on the y-axis. The load line represents the varied loading on the component. As long as the load line remains below the Goodman line *and* the yield line, the component is capable of infinite life.

Component	Max Stress	Min Stress	Mean Stress	Yield Stress	Ult. Strength
Pod Bracket	26640	0	13320	52000	87000
Frame	34750	0	17375	52000	87000
Lock Pin	23070	0	11535	52000	87000
Spring Link	5135	0	2567.5	52000	87000
Handle	30650	0	15325	52000	87000

Table 5: Maximum, Minimum, and Mean Stress Values (psi)

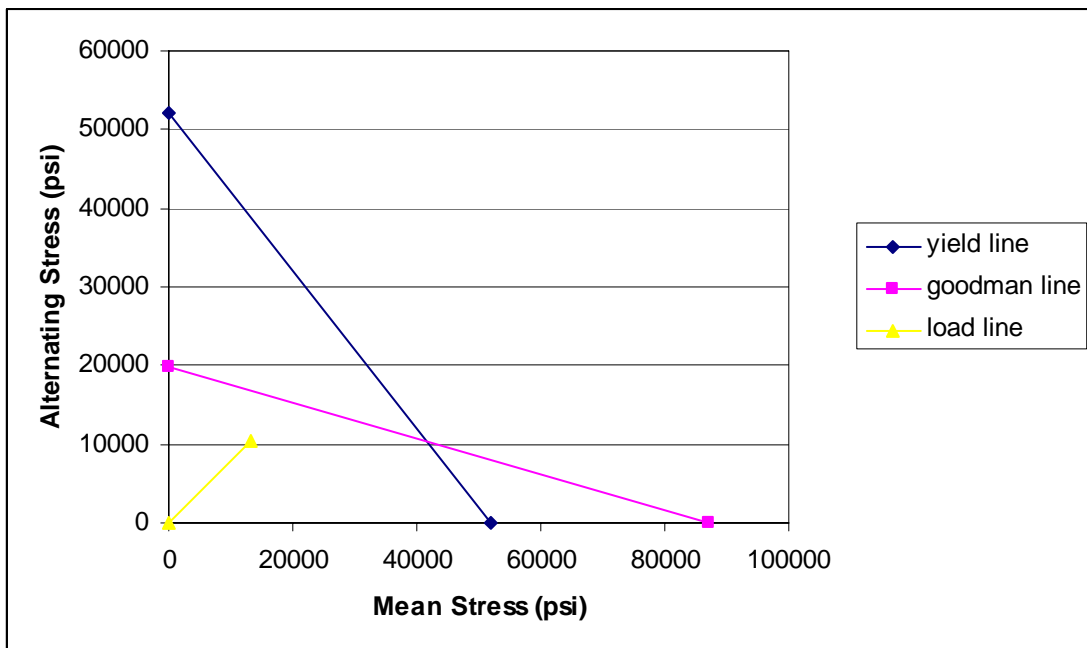


Figure 37: Goodman Diagram of Pod Attachment Bracket

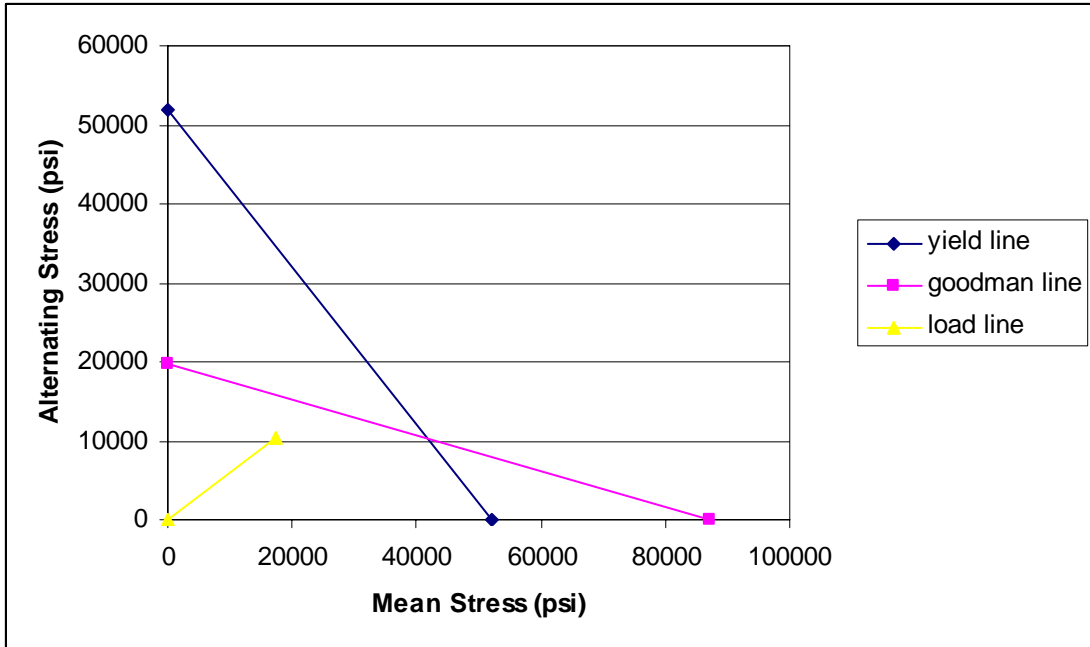


Figure 38: Goodman Diagram of Arm Frame

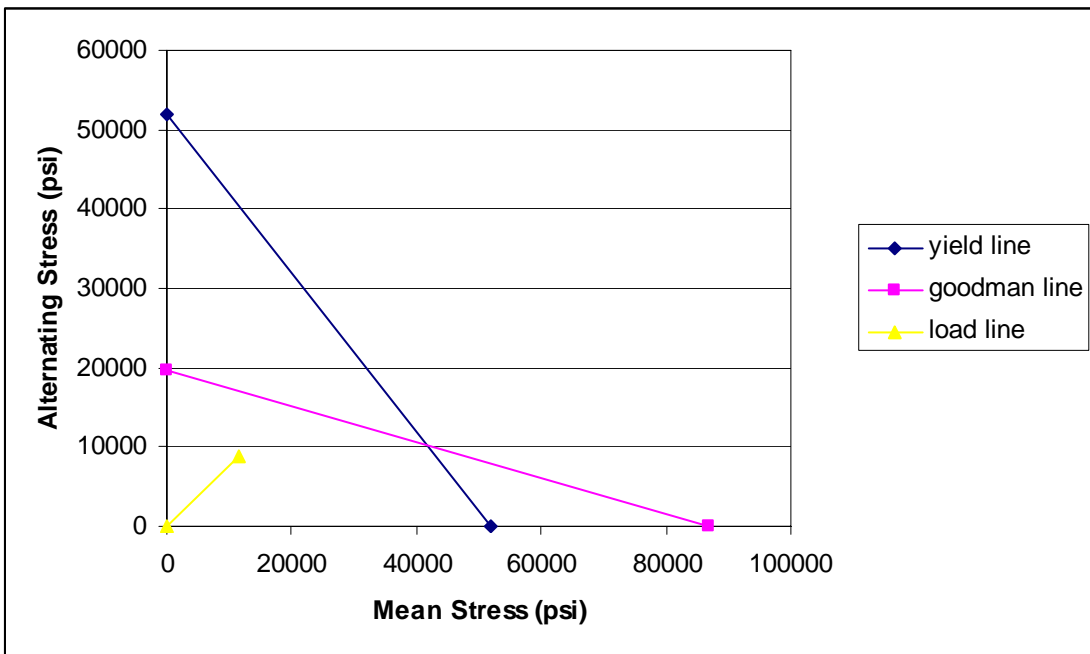


Figure 39: Goodman Diagram of Lock Pin

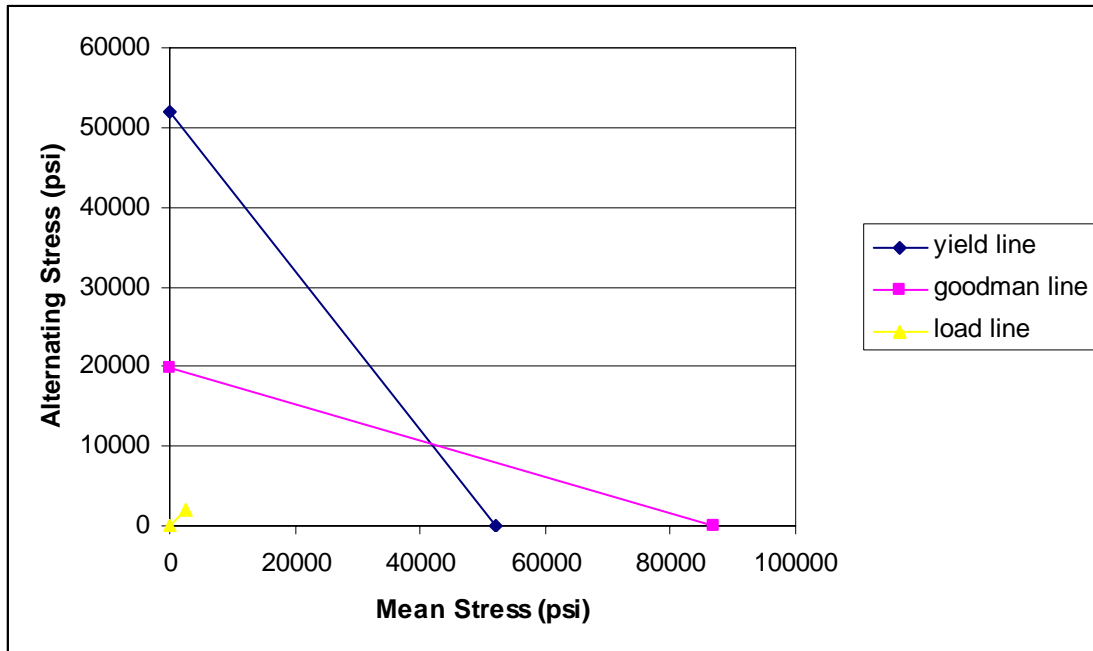


Figure 40: Goodman Diagram of Spring Link

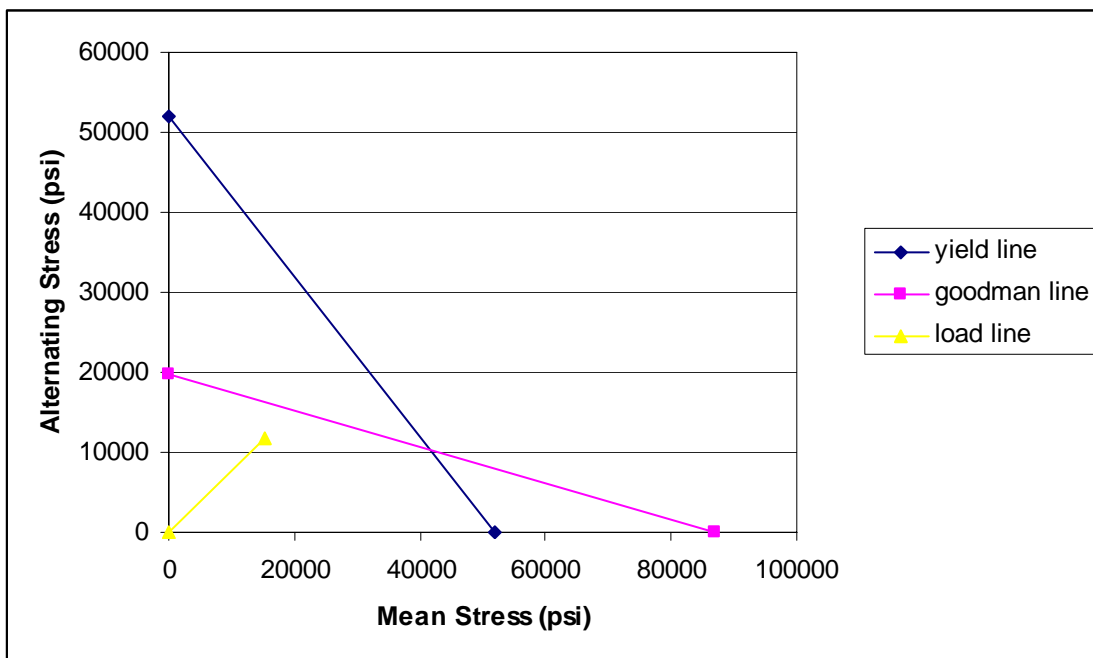


Figure 41: Goodman Diagram of Handle

## **5.0 Results and Conclusions**

The design and analysis discussed in this thesis produced a quick release mechanism for a sensor platform on a C-130 aircraft. The mechanism will allow the sensor platform to be more versatile in that it will allow the sensor-carrying pod to be removed and replaced quickly and easily. The mechanism is simple in its construction and operation, and is easily added to the existing pod/arm configuration. It will fix the pod to the arms in their required position, as in the original configuration. The components of the mechanism possess the strength required to support the pod and its contents. The final design of the mechanism is shown in Figure 42.

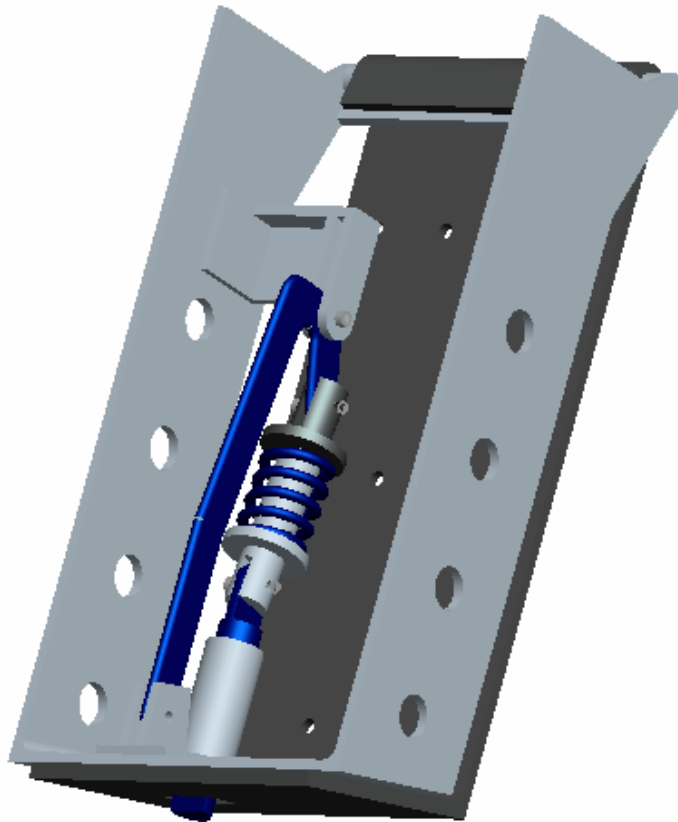


Figure 42: Quick-Release System

## **6.0 Future Work**

Future work on this project will include the construction and implementation of the quick-release mechanism into the current version of the sensor platform. Once the mechanism is incorporated into the sensor platform system, it will need to be tested, reanalyzed, and optimized. After all ground-based testing is finished, flight-testing of the system will need to be performed with a simulated sensor load. The system can then be outfitted with electrical resistance strain gages and analyzed to support the data found in this work.



## **7.0 References**

- 1.) Auld, Jeffery R.X.; Pertl, Emily D.; Smith, James E.; “C<sup>4</sup>ISR System and Remote Sensor Criteria for HLS use of the C-130 Aircraft,” SAE Paper No. 2005-01-0036.
- 2.) Wowczuk, Zenovy S.; Means, Kenneth H.; Mucino, Victor H.; Thompson, Gregory J.; Smith II, James; Auld, Jeffery R.X; Smith, James E.; Naternicola, Adam; Feragotti, Lawrence; Corso, Bruce J.; “Design of a Standardized Roll-On, Roll-Off Sensor Pallet System for a C-130 Aircraft,” SAE Paper No. 2004-01-3092.
- 3.) Feragotti, Lawrence A.; Wowczuk, Zenovy S.; Smith, James E.; “Analysis of the C-130 Sensor Deployment System Arm Using Finite Element Methods,” SAE Paper No. 2004-01 3098.
- 4.) Wowczuk, Zenovy S.; Means, Kenneth H.; Mucino, Victor H.; Thompson, Gregory J.; Feragotti, Lawrence; Smith, James E.; Naternicola, Adam; Corso, Bruce J., “Dynamic Modal Analysis and Optimization of a Mechanical Sensor Arm Deployment System for a C-130 Aircraft,” SAE Paper No. 2004-01-3129.
- 5.) Wowczuk, Zenovy S.; Naternicola, Adam; Smith, James E., “C-130 Sensor Platform Modified Bracing Structure Analysis,” IMAC–XXIII Conference and Exposition on Structural Dynamics (Society for Experimental Mechanics), Paper No. 2005-477.
- 6.) Angle II, Gerald; Pertl, F. Andy; Smith, James E., “Velocity Profile Measurements Under the Ramp of a Lockheed Martin C-130 Aircraft,” SAE Paper No. 2004-01-3099.
- 7.) Wowczuk, Zenovy S.; Angle II, Gerald; Smith, James E., “Crash Analysis of a Command and Control System Deployed on the Rear Ramp of a C-130 Aircraft,” SAE Paper No. 2005-01-0033.
- 8.) Hardin, John W.; Wowczuk, Zenovy S.; Wilhelm, Jay P.; Lowery, Andrew D.; Smith, James E., “Maintenance Issues and Fail Safes of the Oculus Sensor Platform System,” SAE Paper No. 2005-01-0034.
- 9.) Wilhelm, Jay P.; Lowery, Andrew D.; Pertl, Franz A.; Nutter, Roy S.; Smith, James E., “Electromagnetic Compliance Issues of Project Oculus,” SAE Paper No. 2005-01-3394.
- 10.) Auld, Jeffrey R. X.; Pertl, Emily D.; Smith, James E., “Development of a Remote Sensor Deployment System for Expanded C<sup>4</sup>ISR use of the C-130 Aircraft,” SAE Paper No. 2005-01-3395.

- 11.) Williams, Kenneth A.; Wowczuk, Zenovy S.; Lucey, Seth D.; Means, Kenneth H.; Smith, James E., "Hub Connection Simulation of a Sensor Platform System," SAE Paper No. 2005-01-3425.
- 12.) Lucey, Seth D.; Wowczuk, Zenovy S.; Williams, Kenneth A.; Thompson, Eric; Means, Kenneth H.; Kang, Bruce; Smith, James E., "Experimental Stress/Strain Analysis of a Standardized Sensor Platform for a C-130 Aircraft," SAE Paper No. 2005-01-3426.
- 13.) Wowczuk, Zenovy S., "Design of a Standardized Sensor Platform for a C-130 Aircraft," Mechanical and Aerospace Engineering Dept., West Virginia University, Morgantown, WV, 26505, Thesis, 2004.
- 14.) Naternicola, Adam C., "Dynamic Modal Analysis and Optimization of C-130 Project Oculus' Mechanical Arm/Pod Sensor Deployment System Using Finite Element Method," Mechanical and Aerospace Engineering Dept., West Virginia University, Morgantown, WV, 26505, Thesis, 2004.
- 15.) "Federal Aviation Regulations", Part 25, Subpart C, 25.303, Federal Aviation Administration
- 16.) Berger, John G.; Haupt, John R., "Skid Steer Loader Bucket Shaker," U.S. Patent 6,757,992, July 6, 2004.
- 17.) Schurz, James L., "Loader Attachment Quick Coupler Device," U.S. Patent 3,606,052, September 20, 1971.
- 18.) Schmidt, Larry W., "Coupling Assembly," U.S. Patent 6,851,916, February 8, 2005.
- 19.) Matthews, Harry, "Loader Vehicles," U.S. Patent 4,030,624, June 21, 1977.
- 20.) Doering, David Arthur, "Latching Device with Detent," U.S. Patent 5,836,734, November 17, 1998.
- 21.) Mather, Joe M., "Design and Development of 943 Skid Steer Loader," SAE Paper No. 851515.
- 22.) Cochran, Gary L., Seeley, Ronald D., Shelton, Donald G., Stromberg, Gary D., "Implement-coupling assembly for material-handling apparatus," U.S. Patent 4,812,103, March 14, 1989.
- 23.) Hutton, David V., "Fundamentals of Finite Element Analysis," McGraw-Hill Series in Mechanical Engineering, New York 2005.

- 24.) Feragotti, Lawrence A., "Sensitivity Analysis of the C-130 Sensor Deployment System Arm using Finite Element Methods," Mechanical and Aerospace Engineering Dept., West Virginia University, Morgantown, WV, 26505, Thesis, 2004.
- 25.) Bhatti, M. Asghar, "Fundamental Finite Element Analysis and Applications : with Mathematica and Matlab Computations," John Wiley and Sons, Inc., Hoboken, New Jersey 2005.
- 26.) MIL-HDBK-1791, "Designing for International Aerial Delivery in Fixed Wing Aircraft," Military Standard Handbook.

## **Appendix A**

### **Mechanism Analysis Spreadsheet**

The spreadsheet in this appendix contains positions and values of the lengths and forces on the lock pin, spring link, and handle. The position of the handle ranges from unlatched, 0 degrees, to latched, 102.9 degrees. The angle of crank is the position of the handle's connection point in reference to its pivot point. The length of spring link ranges from 5.25 inches in the unlatched position to the pin seated position, to 4.5 inches in the center position, to 4.625 inches in the latched position. The angle of spring link is the angle offset with regard to the vertical, center position, with the center position being 0 degrees. The force on the spring link is the force exerted by the spring due to its amount of deflection. The force on the lock pin is the force exerted by the spring link. The angle of crank to spring link is the angle between the handles connection point and the spring link. The force on the crank is the force on the handles connection point. The force at end of handle is the force needed by the user to latch or unlatch the mechanism.

position of handle	angle of handle	angle of crank	length of spring link	angle of spring link	force of spring link	force on lock pin	angle of crank to spring link	force on crank	force at end of handle
unlatched	0.000	85.870	5.250	22.331	0.000	0.000	71.799	0.000	0.000
	1.000	84.870	5.250	22.298	0.000	0.000	72.832	0.000	0.000
	2.000	83.870	5.250	22.258	0.000	0.000	73.872	0.000	0.000
	3.000	82.870	5.250	22.210	0.000	0.000	74.920	0.000	0.000
	4.000	81.870	5.250	22.156	0.000	0.000	75.974	0.000	0.000
	5.000	80.870	5.250	22.094	0.000	0.000	77.036	0.000	0.000
	6.000	79.870	5.250	22.025	0.000	0.000	78.105	0.000	0.000
	7.000	78.870	5.250	21.949	0.000	0.000	79.181	0.000	0.000
	8.000	77.870	5.250	21.867	0.000	0.000	80.263	0.000	0.000
	9.000	76.870	5.250	21.777	0.000	0.000	81.353	0.000	0.000
	10.000	75.870	5.250	21.680	0.000	0.000	82.450	0.000	0.000
	11.000	74.870	5.250	21.577	0.000	0.000	83.553	0.000	0.000
	12.000	73.870	5.250	21.466	0.000	0.000	84.664	0.000	0.000
	13.000	72.870	5.250	21.349	0.000	0.000	85.781	0.000	0.000
	14.000	71.870	5.250	21.225	0.000	0.000	86.905	0.000	0.000
	15.000	70.870	5.250	21.095	0.000	0.000	88.035	0.000	0.000
	16.000	69.870	5.250	20.958	0.000	0.000	89.172	0.000	0.000
	17.000	68.870	5.250	20.814	0.000	0.000	90.316	0.000	0.000
	18.000	67.870	5.250	20.664	0.000	0.000	91.466	0.000	0.000
	19.000	66.870	5.250	20.508	0.000	0.000	92.622	0.000	0.000
	20.000	65.870	5.250	20.345	0.000	0.000	93.785	0.000	0.000
	21.000	64.870	5.250	20.175	0.000	0.000	94.955	0.000	0.000
	22.000	63.870	5.250	20.000	0.000	0.000	96.130	0.000	0.000
	23.000	62.870	5.250	19.818	0.000	0.000	97.312	0.000	0.000
	24.000	61.870	5.250	19.631	0.000	0.000	98.499	0.000	0.000
	25.000	60.870	5.250	19.437	0.000	0.000	99.693	0.000	0.000
	26.000	59.870	5.250	19.237	0.000	0.000	100.893	0.000	0.000
	27.000	58.870	5.250	19.032	0.000	0.000	102.098	0.000	0.000
	28.000	57.870	5.250	18.821	0.000	0.000	103.309	0.000	0.000
	29.000	56.870	5.250	18.604	0.000	0.000	104.526	0.000	0.000
	30.000	55.870	5.250	18.381	0.000	0.000	105.749	0.000	0.000
	31.000	54.870	5.250	18.153	0.000	0.000	106.977	0.000	0.000
	32.000	53.870	5.250	17.920	0.000	0.000	108.210	0.000	0.000
	33.000	52.870	5.250	17.681	0.000	0.000	109.449	0.000	0.000
	34.000	51.870	5.250	17.437	0.000	0.000	110.693	0.000	0.000
	35.000	50.870	5.250	17.188	0.000	0.000	111.942	0.000	0.000
	36.000	49.870	5.250	16.934	0.000	0.000	113.196	0.000	0.000
	37.000	48.870	5.250	16.675	0.000	0.000	114.455	0.000	0.000
	38.000	47.870	5.250	16.411	0.000	0.000	115.719	0.000	0.000
	39.000	46.870	5.250	16.142	0.000	0.000	116.988	0.000	0.000
	40.000	45.870	5.250	15.869	0.000	0.000	118.261	0.000	0.000
	41.000	44.870	5.250	15.591	0.000	0.000	119.539	0.000	0.000

Table 6: Mechanism Analysis Spreadsheet

position of handle	angle of handle	angle of crank	length of spring link	angle of spring link	force of spring link	force on lock pin	angle of crank to spring link	force on crank	force at end of handle
pin seated	41.820	44.050	5.250	15.359	0.000	0.000	120.591	0.000	0.000
	42.000	43.870	5.245	15.324	5.363	5.172	120.806	4.442	0.740
	43.000	42.870	5.215	15.125	35.155	33.937	122.005	28.779	4.796
	44.000	41.870	5.185	14.918	64.559	62.383	123.212	52.193	8.699
	45.000	40.870	5.156	14.702	93.559	90.495	124.428	74.644	12.441
	46.000	39.870	5.128	14.479	122.138	118.259	125.651	96.095	16.016
	47.000	38.870	5.100	14.248	150.282	145.660	126.882	116.509	19.418
	48.000	37.870	5.072	14.008	177.974	172.681	128.122	135.849	22.641
	49.000	36.870	5.045	13.761	205.199	199.309	129.369	154.081	25.680
	50.000	35.870	5.018	13.505	231.940	225.526	130.625	171.173	28.529
	51.000	34.870	4.992	13.242	258.181	251.316	131.888	187.093	31.182
	52.000	33.870	4.966	12.970	283.907	276.663	133.160	201.812	33.635
	53.000	32.870	4.941	12.691	309.101	301.549	134.439	215.305	35.884
	54.000	31.870	4.916	12.404	333.747	325.958	135.726	227.546	37.924
	55.000	30.870	4.892	12.108	357.831	349.870	137.022	238.515	39.752
	56.000	29.870	4.869	11.805	381.335	373.269	138.325	248.191	41.365
	57.000	28.870	4.846	11.495	404.245	396.137	139.635	256.559	42.760
	58.000	27.870	4.823	11.176	426.545	418.455	140.954	263.607	43.934
	59.000	26.870	4.802	10.851	448.219	440.205	142.279	269.324	44.887
	60.000	25.870	4.781	10.518	469.252	461.368	143.612	273.705	45.617
	61.000	24.870	4.760	10.177	489.630	481.926	144.953	276.747	46.125
	62.000	23.870	4.741	9.830	509.337	501.860	146.300	278.453	46.409
	63.000	22.870	4.722	9.475	528.360	521.152	147.655	278.827	46.471
	64.000	21.870	4.703	9.114	546.684	539.782	149.016	277.880	46.313
	65.000	20.870	4.686	8.746	564.295	557.734	150.384	275.626	45.938
	66.000	19.870	4.669	8.372	581.180	574.987	151.758	272.083	45.347
	67.000	18.870	4.653	7.992	597.326	591.526	153.138	267.273	44.546
	68.000	17.870	4.637	7.605	612.720	607.331	154.525	261.225	43.538
	69.000	16.870	4.623	7.213	627.350	622.386	155.917	253.971	42.328
	70.000	15.870	4.609	6.815	641.204	636.674	157.315	245.546	40.924
	71.000	14.870	4.596	6.412	654.271	650.178	158.718	235.991	39.332
	72.000	13.870	4.583	6.004	666.540	662.884	160.126	225.353	37.559
	73.000	12.870	4.572	5.592	678.001	674.775	161.538	213.682	35.614
	74.000	11.870	4.561	5.174	688.645	685.838	162.956	201.030	33.505
	75.000	10.870	4.552	4.753	698.462	696.059	164.377	187.458	31.243
	76.000	9.870	4.543	4.328	707.443	705.426	165.802	173.027	28.838
	77.000	8.870	4.534	3.900	715.583	713.926	167.230	157.803	26.300
	78.000	7.870	4.527	3.468	722.872	721.548	168.662	141.856	23.643
	79.000	6.870	4.521	3.033	729.306	728.284	170.097	125.259	20.876
	80.000	5.870	4.515	2.596	734.878	734.123	171.534	108.088	18.015
	81.000	4.870	4.510	2.157	739.583	739.059	172.973	90.421	15.070
	82.000	3.870	4.507	1.716	743.417	743.084	174.414	72.339	12.057
	83.000	2.870	4.504	1.274	746.378	746.193	175.856	53.926	8.988
	84.000	1.870	4.502	0.831	748.462	748.383	177.299	35.265	5.877
	85.000	0.870	4.500	0.387	749.667	749.650	178.743	16.442	2.740

Table 6: Mechanism Analysis Spreadsheet (continued)

position of handle	angle of handle	angle of crank	length of spring link	angle of spring link	force of spring link	force on lock pin	angle of crank to spring link	force on crank	force at end of handle
center	85.870	0.000	4.500	0.000	750.000	750.000	180.000	0.002	0.000
	86.000	-0.130	4.500	-0.058	749.993	749.992	179.812	2.460	0.410
	87.000	-1.130	4.501	-0.502	749.438	749.409	178.368	21.347	3.558
	88.000	-2.130	4.502	-0.946	748.004	747.902	176.924	40.136	6.689
	89.000	-3.130	4.504	-1.389	745.692	745.473	175.481	58.740	9.790
	90.000	-4.130	4.507	-1.831	742.504	742.125	174.039	77.076	12.846
	91.000	-5.130	4.512	-2.272	738.443	737.863	172.598	95.057	15.843
	92.000	-6.130	4.516	-2.710	733.512	732.692	171.160	112.603	18.767
	93.000	-7.130	4.522	-3.147	727.716	726.618	169.723	129.632	21.605
	94.000	-8.130	4.529	-3.581	721.059	719.652	168.289	146.068	24.345
	95.000	-9.130	4.536	-4.011	713.548	711.800	166.859	161.833	26.972
	96.000	-10.130	4.545	-4.439	705.189	703.074	165.431	176.858	29.476
	97.000	-11.130	4.554	-4.863	695.989	693.484	164.007	191.072	31.845
	98.000	-12.130	4.564	-5.283	685.957	683.042	162.587	204.411	34.068
	99.000	-13.130	4.575	-5.699	675.100	671.763	161.171	216.813	36.135
	100.000	-14.130	4.587	-6.111	663.428	659.658	159.759	228.221	38.037
	101.000	-15.130	4.599	-6.517	650.950	646.743	158.353	238.582	39.764
	102.000	-16.130	4.612	-6.919	637.677	633.033	156.951	247.846	41.308
latched	102.900	-17.030	4.625	-7.276	625.061	620.028	155.694	255.211	42.535

Table 6: Mechanism Analysis Spreadsheet (continued)

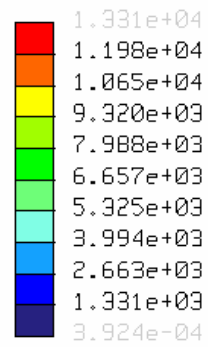
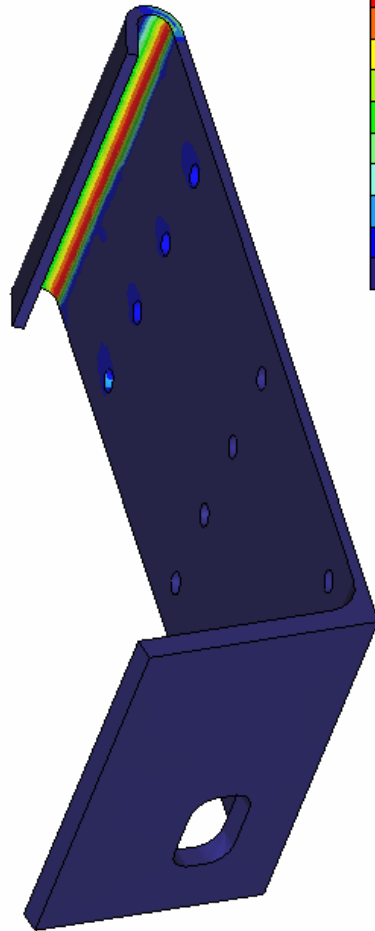
## **Appendix B**

### **Finite Element Analysis Results**

The Finite Element Analysis results in this appendix illustrate the von Mises stresses (in pounds per square inch) and displacement magnitudes (in inches) that occur in the components when subjected to the loading in the Analysis section.



Stress von Mises (WCS)  
(lbf / in<sup>2</sup>)  
Loadset:LoadSetI



Displacement Mag (WCS)  
(in)  
Max Disp +3.5906E-03  
Loadset:LoadSetI

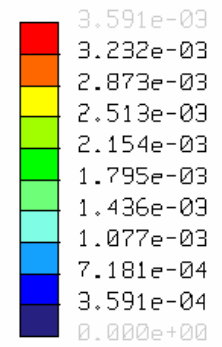
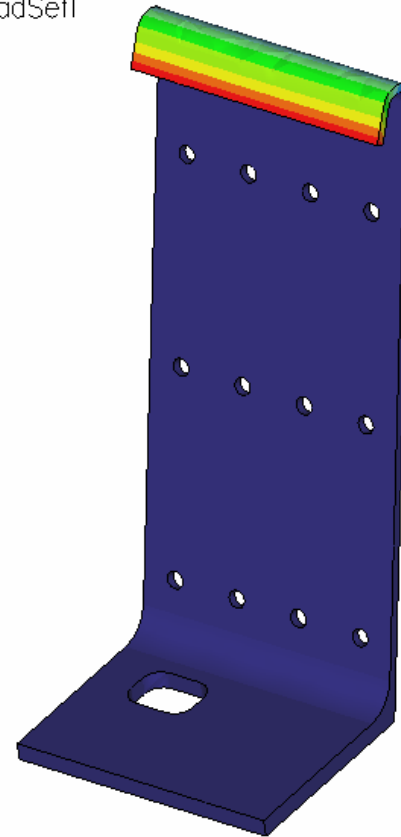
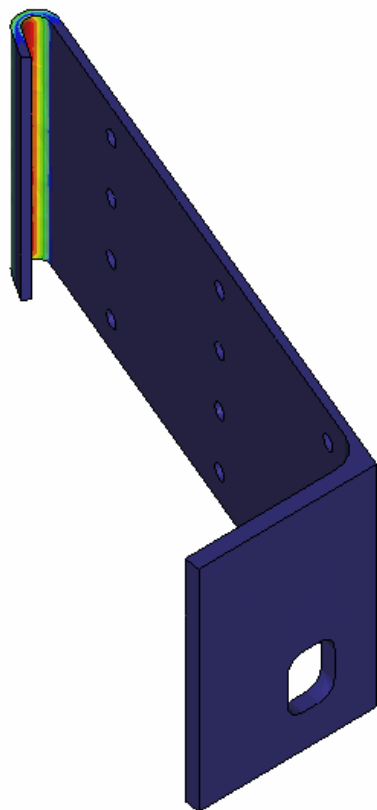
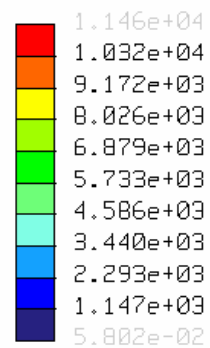


Figure 43: Analysis of Pod Attachment Bracket in the Deployed Position

Stress von Mises (WCS)  
(lbf / in<sup>2</sup>)  
Loadset:LoadSetI



Displacement Mag (WCS)  
(in)  
Max Disp +4.5785E-03  
Loadset:LoadSetI

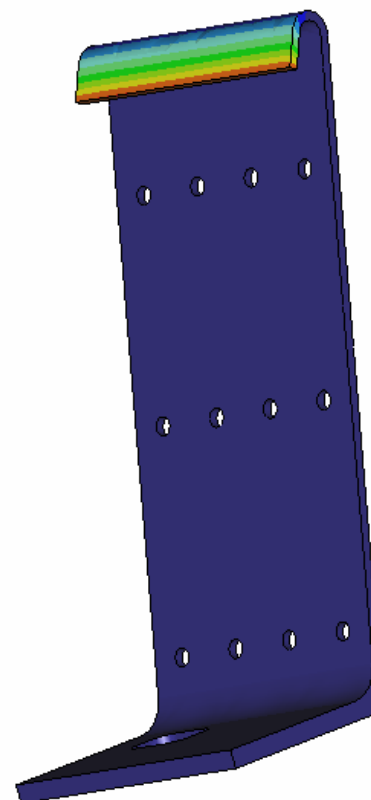
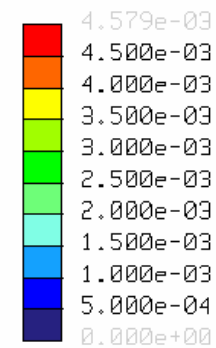
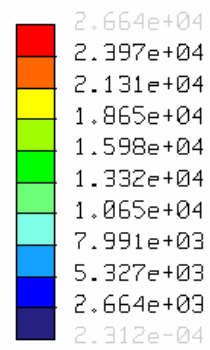
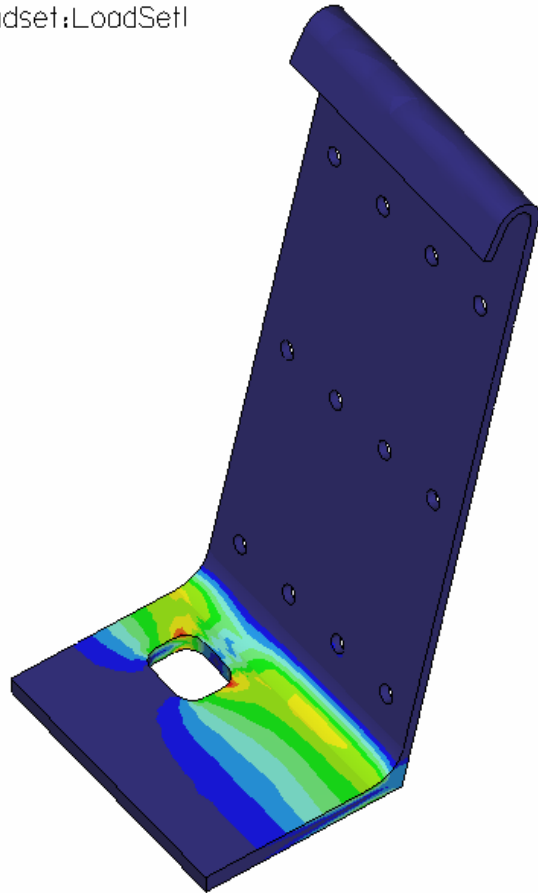


Figure 44: Analysis of Pod Attachment Bracket in the Mid-Deployment Position

Stress von Mises (WCS)  
(lbf / in<sup>2</sup>)  
Loadset:LoadSetI



Displacement Mag (WCS)  
(in)  
Max Disp +2.6307E-02  
Loadset:LoadSetI

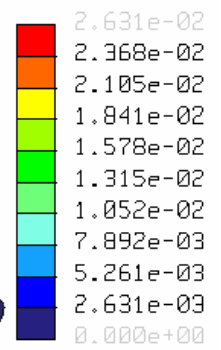
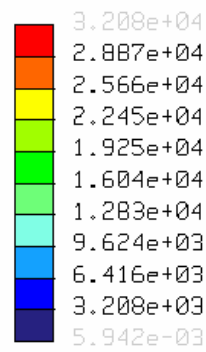
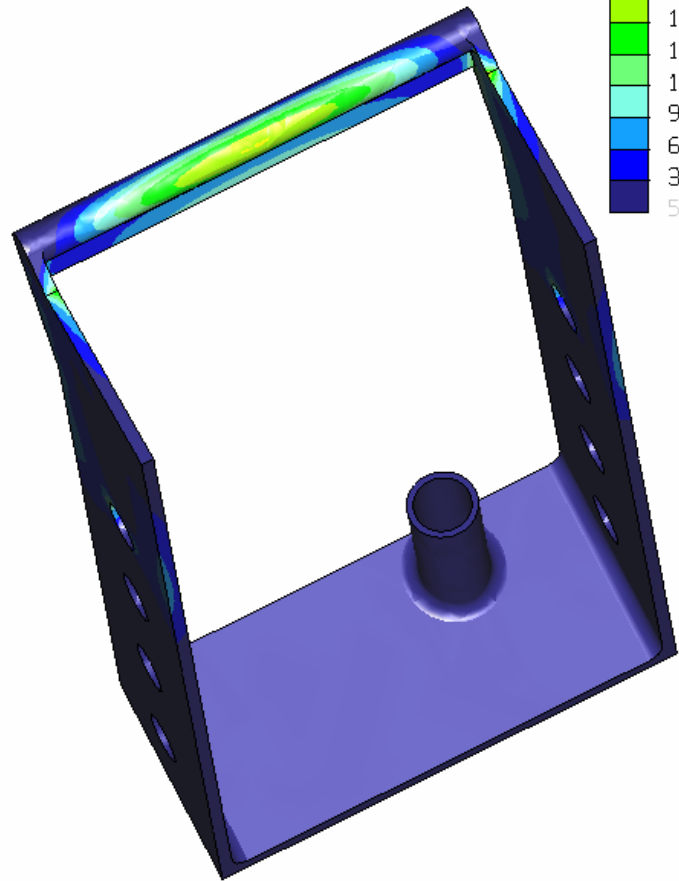


Figure 45: Analysis of Pod Attachment Bracket in the Stowed Position

Stress von Mises (WCS)  
(lbf / in<sup>2</sup>)  
Loadset:LoadSetI



Displacement Mag (WCS)  
(in)  
Max Disp +1.9841E-02  
Loadset:LoadSetI

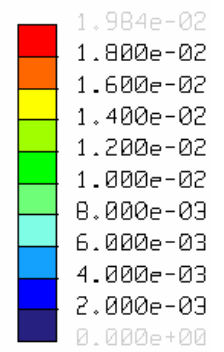
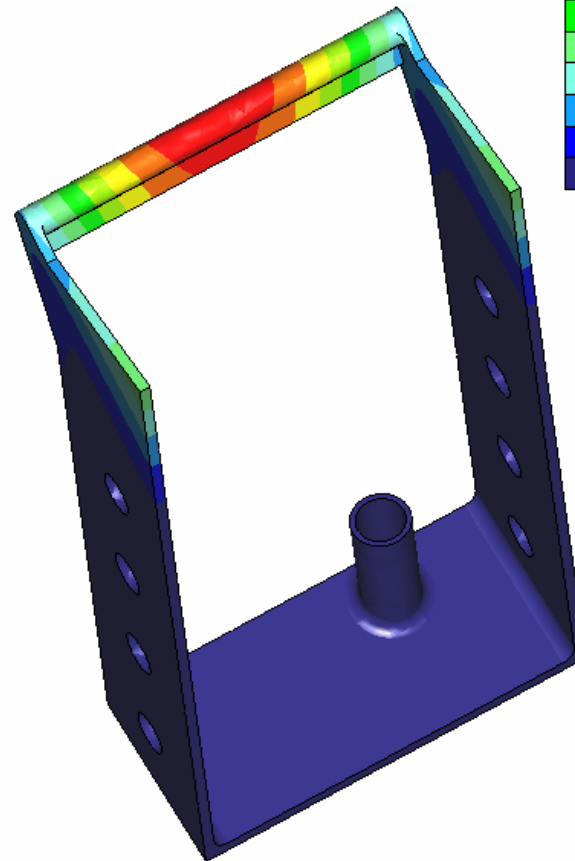


Figure 46: Analysis of Arm Frame in the Deployed Position

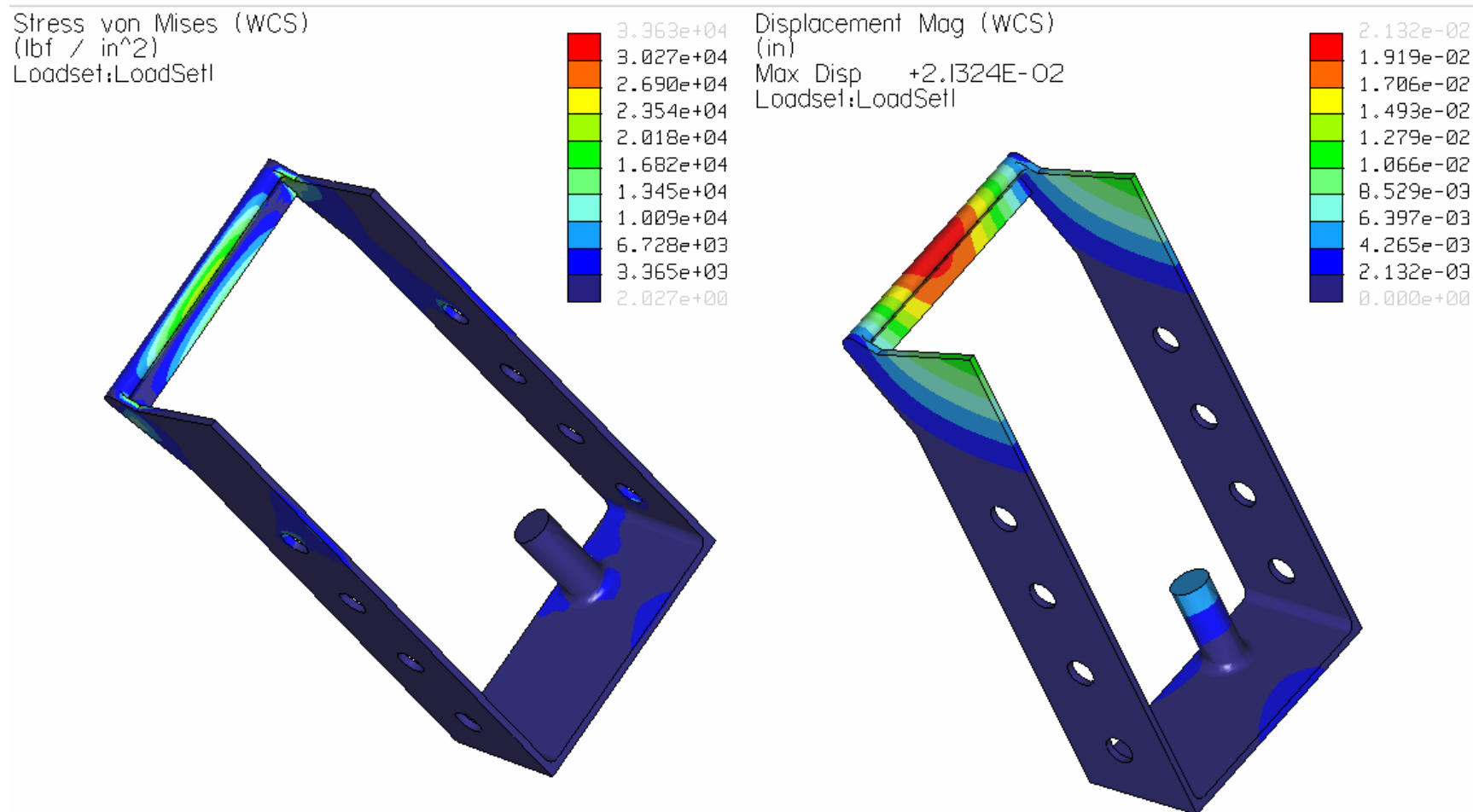


Figure 47: Analysis of Arm Frame in the Mid-Deployment Position

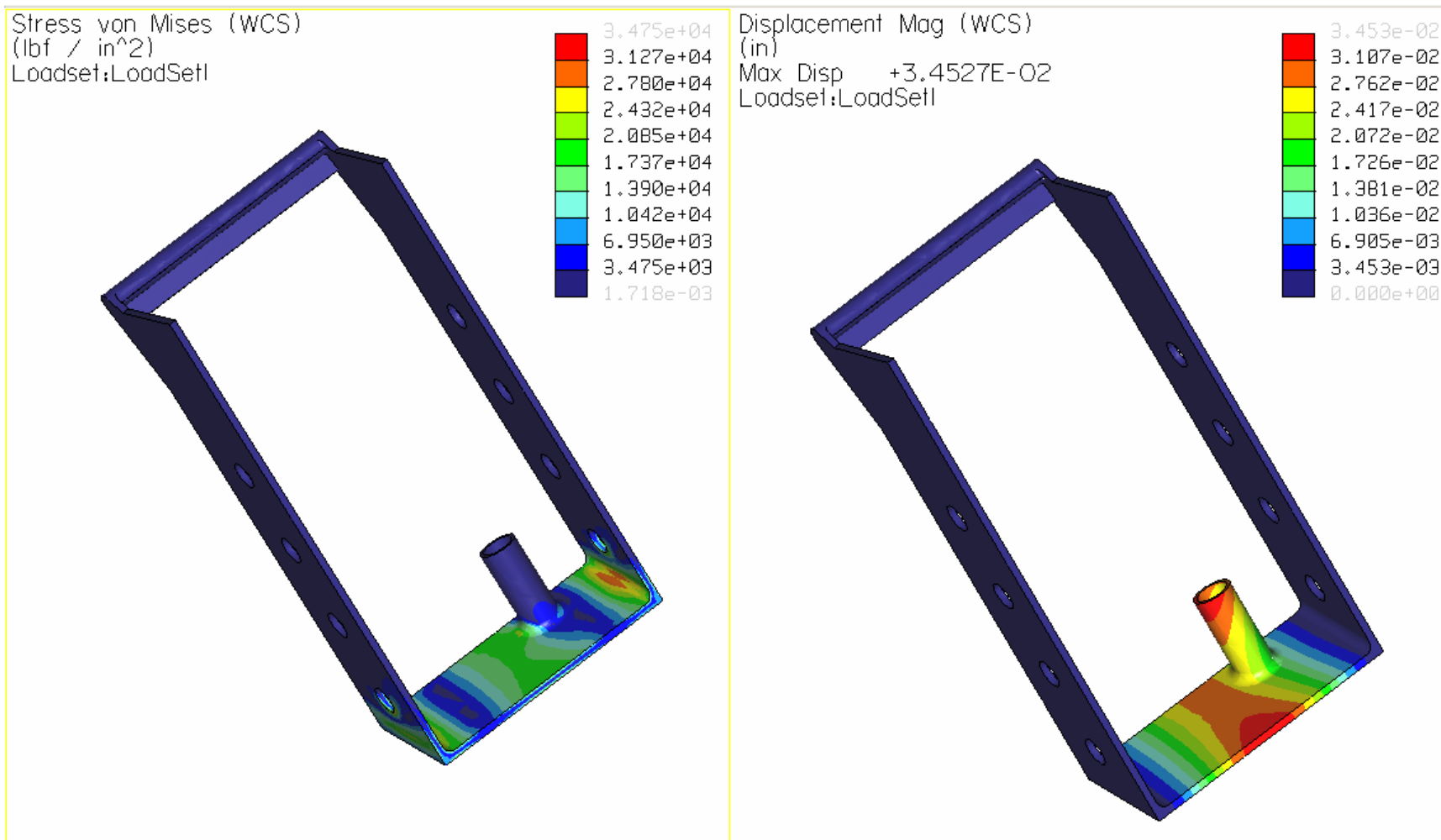
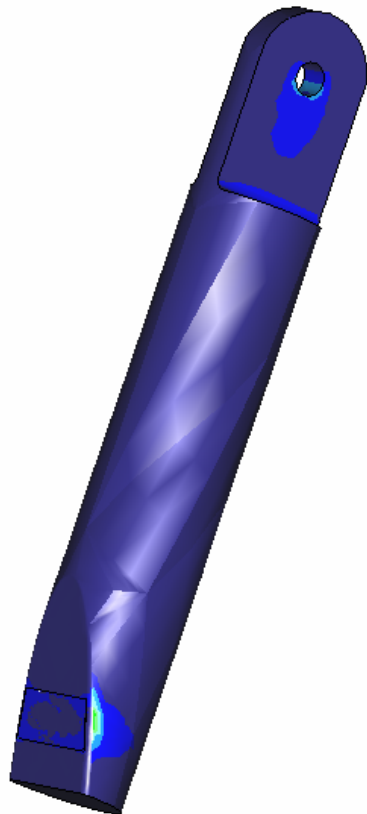
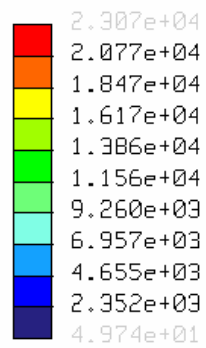


Figure 48: Analysis of Arm Frame in the Stowed Position

Stress von Mises (WCS)  
(lbf / in<sup>2</sup>)  
Loadset:LoadSetI



Displacement Mag (WCS)  
(in)  
Max Disp +2.0739E-04  
Loadset:LoadSetI

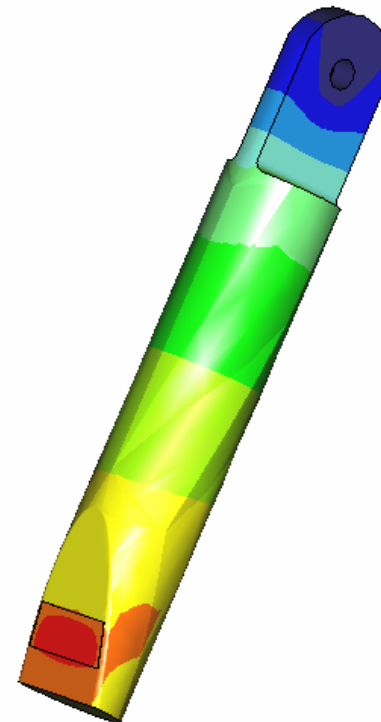
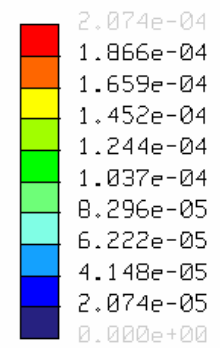
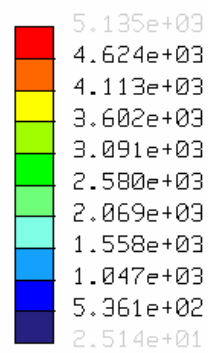
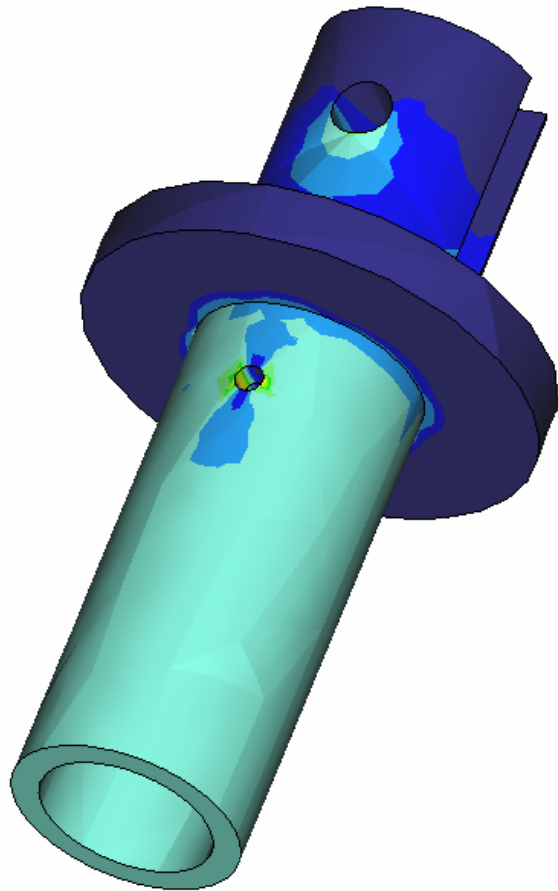


Figure 49: Analysis of Lock Pin in the Mid-Deployment Position

Stress von Mises (WCS)  
(lbf / in<sup>2</sup>)  
Loadset:LoadSetI



Displacement Mag (WCS)  
(in)  
Max Disp +1.6762E-04  
Loadset:LoadSetI

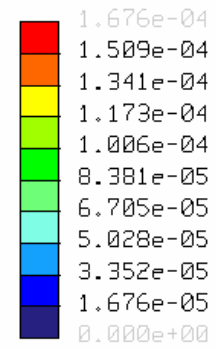
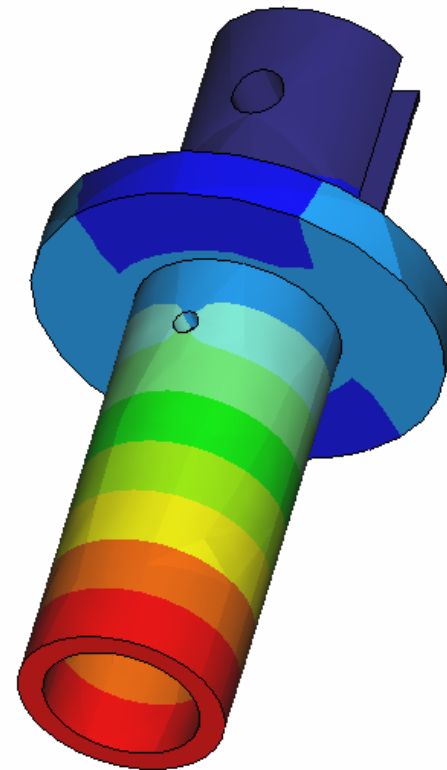
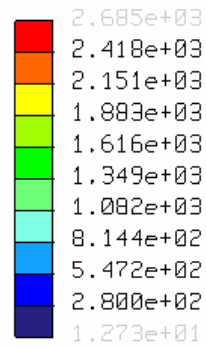
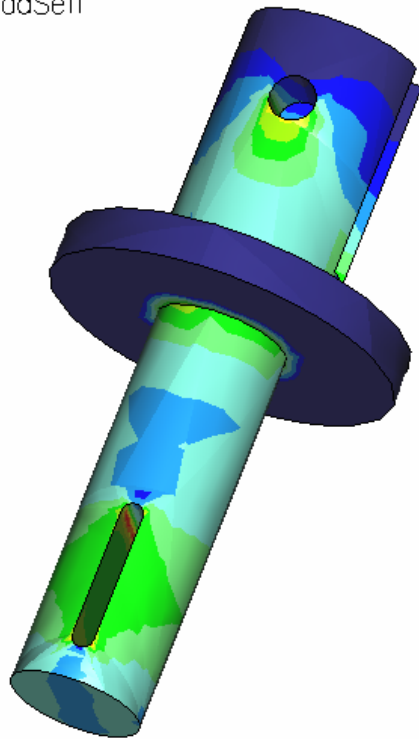


Figure 50: Analysis of Female Component of Spring-Link in the Latched Position



Stress von Mises (WCS)  
(lbf / in<sup>2</sup>)  
Loadset:LoadSetI



Displacement Mag (WCS)  
(in)  
Max Disp +1.4528E-04  
Loadset:LoadSetI

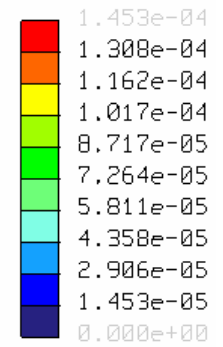
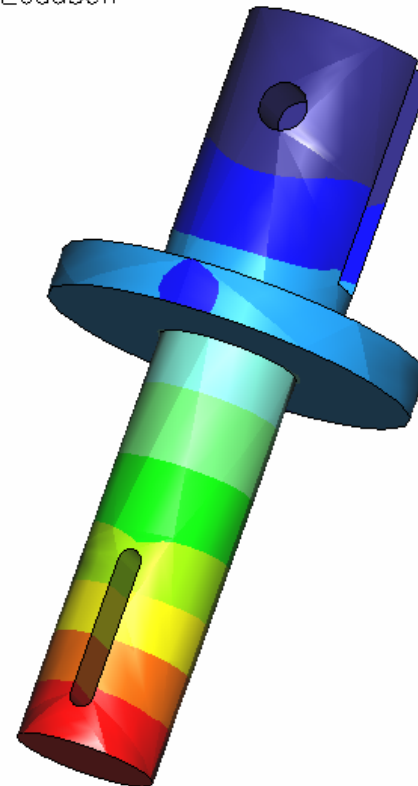
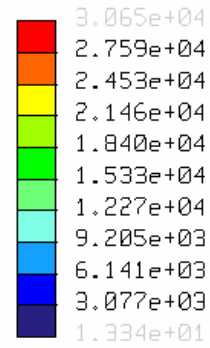


Figure 51: Analysis of Male Component of Spring-Link in the Latched Position

Stress von Mises (WCS)  
(lbf / in<sup>2</sup>)  
Loadset:LoadSetI



Displacement Mag (WCS)  
(in)  
Max Disp +2.6828E-03  
Loadset:LoadSetI

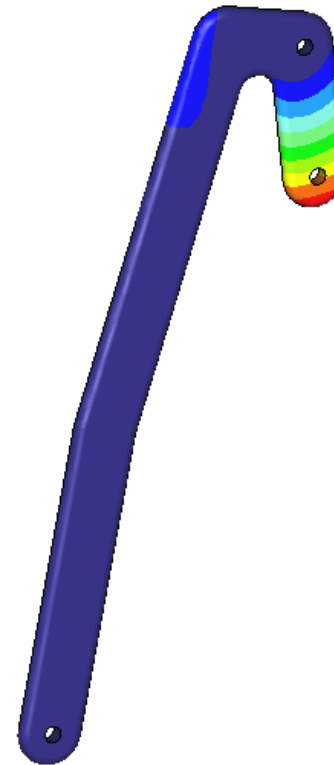
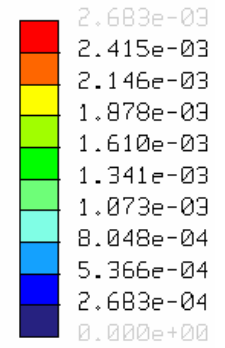


Figure 52: Analysis of Handle in the Latched Position